



# Heat Transport Through an Open Coupled Scalar Field Theory Hosting Stability-to-Instability Transition

T. R. Vishnu<sup>1</sup> · Dibyendu Roy<sup>1</sup>

Received: 26 February 2024 / Accepted: 23 September 2024

© The Author(s), under exclusive licence to Springer Science+Business Media, LLC, part of Springer Nature 2024

## Abstract

We investigate heat transport through a one-dimensional open coupled scalar field theory, depicted as a network of harmonic oscillators connected to thermal baths at the boundaries. The non-Hermitian dynamical matrix of the network undergoes a stability-to-instability transition at the exceptional points as the coupling strength between the scalar fields increases. The open network in the unstable regime, marked by the emergence of inverted oscillator modes, does not acquire a steady state, and the heat conduction is then unbounded for general bath couplings. In this work, we engineer a unique bath coupling where a single bath is connected to two fields at each edge with the same strength. This configuration leads to a finite steady-state heat conduction in the network, even in the unstable regime. We also study general bath couplings, e.g., connecting two fields to two separate baths at each boundary, which shows an exciting signature of approaching the unstable regime for massive fields. We derive analytical expressions for high-temperature classical heat current through the network for different bath couplings at the edges and compare them. Furthermore, we determine the temperature dependence of low-temperature quantum heat current in different cases.

**Keywords** Heat transport · Coupled scalar field theory · Stability-to-instability transition · Quantum Langevin equations

## 1 Introduction

The physics of non-Hermitian quantum systems [1] has received extensive research interest in the last three decades. The first wave of research came through the parity-time ( $PT$ ) symmetric non-Hermitian Hamiltonians, which display real eigenenergies and exhibit exciting comparisons to the dynamics of Hermitian Hamiltonians [2–9]. The topological features

---

Communicated by T. Prosen.

---

T. R. Vishnu and Dibyendu Roy have contributed equally to this work.

---

✉ Dibyendu Roy  
droy@rri.res.in

T. R. Vishnu  
vishnu@rrimail.rri.res.in

<sup>1</sup> Department of Theoretical Physics, Raman Research Institute, Sadashivanagar, Bengaluru, Karnataka 560080, India

of non-Hermitian Hamiltonians with different discrete symmetries [10–18] have generated a second wave of research interest. While the Hermitian Hamiltonian description is valid for an isolated physical system, the non-Hermitian modeling is natural for most systems when they are in contact with one or multiple environments, as in the canonical and grand-canonical descriptions of equilibrium statistical mechanics. There is another interesting class of Hermitian quadratic bosonic Hamiltonians [19, 20] for closed systems, whose dynamics are governed by non-Hermitian Bogoliubov-de Gennes effective Hamiltonians [21–25]. The emergent non-Hermitian effective Hamiltonians can have a generalized  $\mathcal{PT}$  symmetry, which is broken when diagonalisability is lost at exceptional points (EPs) in the parameter space. These EPs mark stability-to-instability transitions between a dynamically stable regime with the unbroken  $\mathcal{PT}$  symmetry and a dynamically unstable regime with the broken  $\mathcal{PT}$  symmetry.

We consider a coupled quantum scalar field theory in one space dimension that exemplifies such a Hermitian quadratic bosonic Hamiltonian. Such field theories have been explored for decades in understanding basic physical phenomena, such as the Higgs field, and introducing novel concepts and techniques of quantum field theories [26, 27]. It is possible to engineer prototypes of such field theories using mechanical, optical, and opto-mechanical networks [28]. In the unstable regime of the coupled scalar field theory or network, it hosts inverted harmonic oscillator [29] modes that have been examined for a diverse set of physical phenomena, including the Hawking–Unruh effect and scattering in the lowest Landau level in quantum Hall systems [30]. Here, we connect the two boundaries of the coupled scalar field theory discretized on a lattice as an oscillator network to heat baths kept at different temperatures. We investigate heat transport [31, 32] in this open network. Our motivation is to understand how heat transport behaves around the EPs marking stability-to-instability transitions [33]. To study heat transport, we write quantum Langevin equations for the degrees of freedom of the scalar field theory after integrating out the baths, and solve these equations using the non-equilibrium Green's functions [32, 34]. The steady-state heat transport emerges only in the dynamically stable regime of the field theory for general system-bath coupling due to the appearance of unbounded inverted oscillator modes in the unstable regime. Nevertheless, as explained in our study, heat transport is insensitive to stability-to-instability transition for some particular types of bath couplings, which is one of our main findings. We derive analytical expressions for the heat current in the high-temperature linear response regime and evaluate the temperature dependence of quantum heat current. The temperature dependence is different for the massive and massless scalar fields and it also depends on the bath coupling and the coupling between the scalar fields. We further compare steady-state heat transport between different types of bath couplings at two boundaries and between separate heat bath spectral properties. Heat current for general bath couplings, e.g., connecting two fields to two separate baths at each boundary, shows an exciting signature of approaching the unstable regime for massive scalar fields.

The rest of the paper is divided into six sections and four appendices. We introduce the non-Hermitian description for the dynamical matrix of the coupled scalar field theory and the stability-to-instability transition in Sect. 2. In Sect. 3, we introduce a lattice version of the field theory and its spectral properties. The heat conduction through the lattice of oscillators, connected differently to heat baths at the boundaries is discussed in Sect. 4. We include our results for single and two baths at each edge in Sects. 5 and 6, respectively. We conclude with a summary and outlook in Sect. 7. Details of our derivation of heat current for two different bath couplings and different bath spectral properties are included in the four appendices at the end.

## 2 Dynamical Matrix and Stability-to-Instability Transition

We consider a coupled quantum scalar field theory of two real scalar fields  $\phi_1(x)$  and  $\phi_2(x)$  with a minimal coupling represented by the Hamiltonian:

$$\mathcal{H} = \frac{1}{2} \int dx \left[ \Pi_1^2 + c^2 (\partial_x \phi_1)^2 + \Pi_2^2 + c^2 (\partial_x \phi_2)^2 + \frac{m^2 c^4}{\hbar^2} (\phi_1^2 + \phi_2^2) \right] + \lambda c^2 \int dx (\partial_x \phi_1)(\partial_x \phi_2), \quad (1)$$

where the field variables satisfy the usual canonical commutation relations,  $[\phi_\alpha(x), \Pi_\beta(x')] = i\hbar \delta_{\alpha\beta} \delta(x - x')$  for  $\alpha, \beta = 1, 2$ . Here,  $\lambda > 0$  is a dimensionless coupling constant and  $m$  is the mass of the fields. We write down the Heisenberg equations for  $\phi_\alpha$ ,  $\Pi_\alpha$ , and then take Fourier transformation to momentum space as  $\tilde{\phi}_\alpha(q, t) = (1/\sqrt{2\pi}) \int dx e^{-iqx/\hbar} \phi_\alpha(x, t)$  and  $\tilde{\Pi}_\alpha(q, t) = (1/\sqrt{2\pi}) \int dx e^{-iqx/\hbar} \Pi_\alpha(x, t)$  for  $\alpha = 1, 2$  to find

$$i \frac{\partial \hat{\phi}}{\partial t} = i \begin{bmatrix} 0 & 1 & 0 & 0 \\ \frac{-m^2 c^4 - q^2 c^2}{\hbar^2} & 0 & \frac{-\lambda q^2 c^2}{\hbar^2} & 0 \\ 0 & 0 & 0 & 1 \\ \frac{-\lambda q^2 c^2}{\hbar^2} & 0 & \frac{-m^2 c^4 - q^2 c^2}{\hbar^2} & 0 \end{bmatrix} \hat{\phi} \equiv G \hat{\phi}, \quad (2)$$

where  $\hat{\phi} = (\tilde{\phi}_1, \tilde{\Pi}_1, \tilde{\phi}_2, \tilde{\Pi}_2)^T$ . The matrix  $G$  governs the dynamics of these field variables. In general, the dynamical matrix  $G$  is non-Hermitian, i.e.  $G \neq G^\dagger$ . In fact, we find,  $G^\dagger = \tau_2 G \tau_2$ , where  $\tau_2 = \mathbf{1}_2 \otimes \sigma_2$ ; thus,  $G$  is a pseudo-Hermitian matrix. Here,  $\mathbf{1}_2$  is a  $2 \times 2$  identity matrix and  $\sigma_i$ 's (for  $i = 1, 2, 3$ ) are Pauli matrices.

The eigenvalues of  $G$  are  $\pm(c/\hbar)\sqrt{c^2 m^2 + q^2(1 \pm \lambda)}$ . For fixed values of  $q$  and  $m$ , the eigenvalues of  $G$  switch from real to complex conjugate pairs as we change  $\lambda$  beyond  $1 + (cm/q)^2 \equiv 1 + (k_C/k)^2$ , where the Compton wave number  $k_C = mc/\hbar$  and momentum  $q = \hbar k$ . Then, the transition from real to complex eigenvalues of  $G$  results for wave number  $k^2 > k_C^2/(\lambda - 1)$ . Thus, for sufficiently high frequencies, the condition  $\lambda > 1$  leads to an ultra-violet instability. When the eigenvalues become zero for some parameters, the eigenvectors also coincide. These values of parameters correspond to EPs in the parameter-space. The generalized  $\mathcal{PT}$  symmetry of  $G$  explains these features of the eigenvalues. In fact, we find,  $G^* = \tau_3 G \tau_3$  for  $\tau_3 = \mathbf{1}_2 \otimes \sigma_3$ , which is in general, true for any  $\mathcal{PT}$  symmetric matrix. Let us consider,

$$[\mathcal{PT}, G] = 0 \implies \mathcal{P}G^* = GP. \quad (3)$$

Thus,  $G$  is  $\mathcal{PT}$  symmetric matrix when we identify the parity operator as  $\mathcal{P} = \tau_3$ . In general, a non-Hermitian (Hamiltonian) matrix admits a real spectrum for some values of the parameter even if the symmetry operator is not  $\mathcal{PT}$ , but instead is an anti-unitary operator  $A$  satisfying the condition  $A^{2r} = 1$  with  $r$  odd [6]. In fact, this is known as the generalized  $\mathcal{PT}$ -symmetry. The unbroken regime of symmetry admits real spectrum while the spontaneous breaking of the symmetry leads to complex eigenvalues. To understand the symmetry of  $G$  better, we notice that a combination of  $\tau_3$  and complex conjugation operator  $\kappa$  acts as the anti-unitary operator  $A = \tau_3 \kappa$ . Here,  $\kappa$  acts as a time-reversal operator ( $\mathcal{T}$ ) for spin-less systems. The spectrum of the Hermitian Hamiltonian in Eq. 1 also drastically changes its features across the EPs.

### 3 Coupled Scalar Field Theory on Lattice: Two-Component Harmonic Chain

We discretize this field theory by placing it on a lattice enabling the calculation of non-equilibrium heat transport using the lattice Green’s functions. We use the redefinition,  $y_{\alpha,n} = (cd^2/\hbar)^{1/2}\phi_{\alpha}(x = nd)$ ,  $p_{\alpha,n} = (\hbar/c)^{1/2}\Pi_{\alpha}(x = nd)$  for  $\alpha = 1, 2$  and  $n = 1, 2, \dots, N$ . Here,  $d$  is the lattice spacing. Thus, the effective low-energy (since  $d$  introduces a UV cutoff) description of this field theory in Eq. 1 is given by the Hamiltonian:

$$H = \sum_{\alpha=1}^2 \left[ \sum_{n=1}^N \left( \frac{p_{\alpha,n}^2}{2m_0} + \frac{k_p}{2} y_{\alpha,n}^2 \right) + \sum_{n=0}^N \frac{k}{2} (y_{\alpha,n+1} - y_{\alpha,n})^2 \right] + \lambda k \sum_{n=0}^N (y_{1,n+1} - y_{1,n})(y_{2,n+1} - y_{2,n}). \tag{4}$$

Here,  $m_0 = \hbar/dc$ ,  $k_p = (\hbar/dc)(m^2c^4/\hbar^2)$  and  $k = (\hbar/dc)(c/d)^2$ . Physically, this Hamiltonian represents a network made by a pair of interconnected chains of harmonic oscillators (springs) representing two types of scalar fields. We have  $[y_{\alpha,n}, p_{\beta,n'}] = i\hbar\delta_{nn'}\delta_{\alpha\beta}$ . We may view this network as a two-component harmonic oscillator chain. In other words, the same kind of oscillators are connected to their nearest neighbors by spring constant  $k$ . The chains are coupled between each other through a coupling  $\lambda k$ . Moreover, each oscillator is locally pinned by a harmonic potential of strength  $k_p$ . We impose fixed boundary conditions,  $y_{\alpha,0} = y_{\alpha,N+1} = 0$  for the network. The Hamiltonian in Eq. 4 can be diagonalized by a series of transformations to normal modes:  $y_{\alpha,n} = \sqrt{2/(N+1)} \sum_{q'=1}^N \tilde{y}_{\alpha,q'} \sin[\pi nq'/(N+1)]$ ,  $\tilde{y}_{s/a,q'} = (\tilde{y}_{1,q'} \pm \tilde{y}_{2,q'})/\sqrt{2}$ , and similar relations for  $p_{\alpha,n}$ . Thus, we get

$$H = \sum_{q'=1}^N \left[ \frac{\tilde{p}_{s,q'}^2}{2m_0} + \frac{m_0\Omega_{s,q'}^2}{2} \tilde{y}_{s,q'}^2 + \frac{\tilde{p}_{a,q'}^2}{2m_0} + \frac{m_0\Omega_{a,q'}^2}{2} \tilde{y}_{a,q'}^2 \right], \tag{5}$$

where the frequencies  $\Omega_{s,q'}$ ,  $\Omega_{a,q'}$  of symmetric and anti-symmetric normal modes are,  $\Omega_{s/a,q'}^2 = (k_p/m_0) + (4k(1 \pm \lambda)/m_0) \sin^2[\pi q'/(2(N+1))]$ . For  $\lambda > \lambda_c \equiv 1 + (k_p/4k) \csc^2[\pi N/(2(N+1))]$ ,  $\Omega_{a,q'}$  can become imaginary implying the presence of inverted oscillator modes along with regular oscillators. Thus, the network can admit imaginary frequencies beyond a critical  $\lambda$ , which leads to an instability in the field theory. The evolution of some observables, e.g., the out-of-time order correlators (OTOC), is unbounded in time in the dynamically unstable regime for parameters with at least one inverted normal mode [35–37]. In the absence of inverted normal modes, the time evolution of all observables including the OTOC is bounded in the dynamically stable regime.

### 4 Heat Conduction

We connect two ends of the oscillator network to heat baths kept at different temperatures  $T_L, T_R$ . We consider two different types of coupling between the network and the baths at the boundaries. We first take both the oscillators (fields) at any boundary being connected to a single bath with the same coupling strength (see Fig. 1). This leads to the equations of motion (EOM) for the oscillators at the boundaries in the following form for any general model of baths:

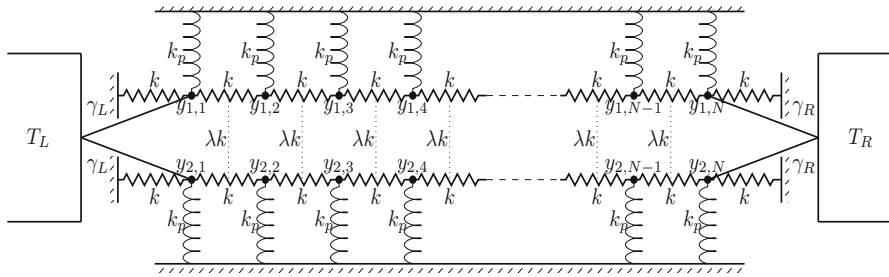


**Fig. 1** A cartoon of the oscillator network connected to a single bath at each boundary. Here,  $T_L$  and  $T_R$  denote the left and right bath temperatures, respectively. The parameters  $k$ ,  $k_p$  and  $\lambda k$ , respectively, represent the spring constant, local pinning strength, and coupling strength between the two types of oscillator chains. The bath coupling with the network at the left and right boundary are  $\gamma_L$  and  $\gamma_R$ , respectively

$$m_0 \ddot{y}_{\alpha,1} = -k_p y_{\alpha,1} - k \left[ (2y_{\alpha,1} - y_{\alpha,2}) + \lambda (2y_{\beta,1} - y_{\beta,2}) \right] + \int_{-\infty}^t dt' \Sigma_L^+(t-t') \sqrt{2} y_{s,1}(t') + \eta_L, \tag{6}$$

$$m_0 \ddot{y}_{\alpha,N} = -k_p y_{\alpha,N} - k \left[ (2y_{\alpha,N} - y_{\alpha,N-1}) + \lambda (2y_{\beta,N} - y_{\beta,N-1}) \right] + \int_{-\infty}^t dt' \Sigma_R^+(t-t') \sqrt{2} y_{s,N}(t') + \eta_R, \tag{7}$$

where  $\alpha \neq \beta$ ,  $\alpha, \beta = 1, 2$ , and the symmetric modes  $y_{s,n}(t) = (y_{1,n}(t) + y_{2,n}(t))/\sqrt{2}$  for  $n = 1, 2, \dots, N$ . Here, we assume the heat baths are connected to the network at infinite past. The noise terms  $\eta_L(t)$ ,  $\eta_R(t)$  from the left and right heat baths are related to the self energies  $\Sigma_L^+$ ,  $\Sigma_R^+$  of the corresponding baths through the fluctuation-dissipation relations as given in Eq. 20.

The heat current in the network can be evaluated by calculating the rate at which the heat bath at any boundary does work on the network [34, 38]. Employing the continuity equation, we find the heat current  $J_1(t)$  at the left boundary as

$$J_1(t) = -\dot{y}_{s,1}(t) (\sqrt{2} \eta_L(t) + \int_{-\infty}^t dt' 2 \Sigma_L^+(t-t') y_{s,1}(t')), \tag{8}$$

which solely depends on the symmetric modes of the network. Such form of heat current appears due to the symmetric coupling of the heat baths with the network, which is also evident from the EOM for the oscillators at the boundaries in Eqs. 6 and 7. Since the frequency of the symmetric modes remains real-valued for all  $\lambda$ , these modes are bounded for all time. Therefore,  $J_1(t)$  is insensitive to the stability-to-instability transition in the network for symmetric connections to one heat bath at each boundary. We can find a steady state of  $J_1(t)$  both in the stable and unstable regime of the network.

Next, we consider that each oscillator (field) at any boundary is connected to an individual heat bath with the same coupling strength (see Fig. 2). Both baths at any boundary are kept at the same temperature. Such coupling leads to the EOM for the oscillators at the boundaries in the following form for a general model of heat baths:

$$m_0 \ddot{y}_{\alpha,1} = -k_p y_{\alpha,1} - k \left[ (2y_{\alpha,1} - y_{\alpha,2}) + \lambda (2y_{\beta,1} - y_{\beta,2}) \right] + \int_{-\infty}^t dt' \Sigma_{\alpha,L}^+(t-t') y_{\alpha,1}(t') + \eta_{\alpha,L}, \tag{9}$$

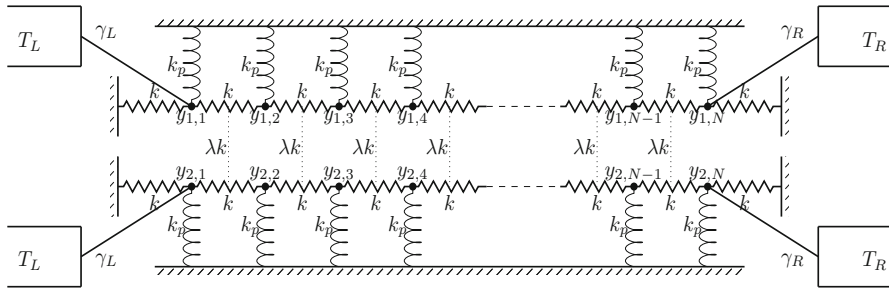


**Fig. 2** A cartoon of the oscillator network connected to two baths at each boundary. Both baths on the left are kept at temperature  $T_L$ , and those at the right are at  $T_R$ , respectively. As explained in Fig. 1, the parameters  $k$ ,  $k_p$ , and  $\lambda k$  represent spring constant, pinning strength, and coupling between the harmonic oscillator chains. The bath coupling with the network at the left and right boundary are  $\gamma_L$  and  $\gamma_R$ , respectively

$$m_0 \ddot{y}_{\alpha,N} = -k_p y_{\alpha,N} - k \left[ (2y_{\alpha,N} - y_{\alpha,N-1}) + \lambda(2y_{\beta,N} - y_{\beta,N-1}) \right] + \int_{-\infty}^t dt' \Sigma_{\alpha,R}^+(t-t') y_{\alpha,N}(t') + \eta_{\alpha,R}, \tag{10}$$

where again  $\alpha \neq \beta$ ,  $\alpha, \beta = 1, 2$ , and  $\eta_{\alpha,L}$  ( $\eta_{\alpha,R}$ ) and  $\Sigma_{\alpha,L}^+$  ( $\Sigma_{\alpha,R}^+$ ) are noise and self-energy of the two heat baths at the left (right) boundary. The heat current  $J_{\Pi}(t)$  for this case from the continuity equation takes the following form at the left boundary:

$$J_{\Pi}(t) = - \sum_{\alpha=1,2} \dot{y}_{\alpha,1}(t) \left( \eta_{\alpha,L}(t) + \int_{-\infty}^t dt' \Sigma_{\alpha,L}^+(t-t') y_{\alpha,1}(t') \right), \tag{11}$$

which shows that both boundary oscillators appear explicitly in the heat current. Thus,  $J_{\Pi}(t)$  depends on both the symmetric and anti-symmetric modes. Consequently,  $J_{\Pi}(t)$  would not reach a steady state for the network in the unstable regime, as the anti-symmetric modes become unbounded over time. Nevertheless,  $J_{\Pi}(t)$  acquires a steady-state value when the network is in the stable regime, since both the symmetric and anti-symmetric modes are bounded over time.

The qualitative difference in achieving steady-state heat conduction due to different ways of coupling to varying numbers of thermal baths at the boundaries is one highlight of our present study. The differences in the system-size scaling of heat conduction for different types of boundary coupling with a fixed number of baths have been shown earlier in heat transport through disordered harmonic lattices, which attracted much attention [39–41]. We consider two different types of heat baths, namely, (a) baths modeled by semi-infinite ordered harmonic chains (Rubin model of baths) [42], and (b) white noise baths [43]. The white noise in a bath is uncorrelated at any two different times signaling Markovian dynamics. The color noise in the Rubin model of bath are correlated for different times indicating non-Markovian feature.

The EOM for the oscillators’ displacements in the bulk for  $\alpha \neq \beta$ ,  $\alpha, \beta = 1, 2$  and  $n = 2, 3, \dots, N - 1$  are:

$$m_0 \ddot{y}_{\alpha,n} = -k_p y_{\alpha,n} - k \left[ (2y_{\alpha,n} - y_{\alpha,n-1} - y_{\alpha,n+1}) + \lambda(2y_{\beta,n} - y_{\beta,n-1} - y_{\beta,n+1}) \right]. \tag{12}$$

We solve these EOM in Eqs. 6, 7, 9, 10, and 12 using Fourier transforms of  $y_{\alpha,n}(t)$ ,  $\eta_b(t)$ ,  $\eta_{\alpha,b}(t)$ ,  $\Sigma_b^+(t)$ ,  $\Sigma_{\alpha,b}^+(t)$  to frequency domain with  $b = L, R$ , e.g.,

$$\tilde{y}_{\alpha,n}(\omega) = \frac{1}{2\pi} \int_{-\infty}^{\infty} dt y_{\alpha,n}(t)e^{i\omega t}. \tag{13}$$

The self-energy  $\tilde{\Sigma}_b^+(\omega) = i\gamma_b^o\omega$  for the white noise baths, and

$$\tilde{\Sigma}_b^+(\omega) = \frac{\gamma_b^2}{k_0} \left[ \left( 1 - \frac{m_0\omega^2}{2k_0} \right) + i \left( \frac{\omega\sqrt{m_0}}{\sqrt{k_0}} \sqrt{1 - \frac{m_0\omega^2}{4k_0}} \right) \right], \tag{14}$$

for the Rubin baths, where  $\gamma_L^o, \gamma_R^o, \gamma_L$ , and  $\gamma_R$  control the coupling of the respective boundary oscillators with the left and right Ohmic and Rubin baths, respectively. This leads to  $\tilde{\Sigma}_{\alpha,b}^+(\omega) = \tilde{\Sigma}_b^+(\omega)$  for  $\alpha = 1, 2$ . Here,  $2\sqrt{k_0}$  is the finite band-width of the Rubin baths in comparison to infinite band width for the white noise baths. We further introduce the symmetric and anti-symmetric modes as  $\tilde{y}_{s/a,n}(\omega) = (\tilde{y}_{1,n}(\omega) \pm \tilde{y}_{2,n}(\omega))/\sqrt{2}$ .

### 5 Single Bath at Each Boundary

For a single bath at each boundary of the network, the EOM in Eqs. 6 and 7 get decoupled in terms of these symmetric and anti-symmetric modes as,

$$z_{L+}\tilde{y}_{s,1}(\omega) - k(1 + \lambda)\tilde{y}_{s,2}(\omega) = \sqrt{2}\tilde{\eta}_L(\omega), \tag{15}$$

$$z_{-}\tilde{y}_{a,1}(\omega) - k(1 - \lambda)\tilde{y}_{a,2}(\omega) = 0, \tag{16}$$

$$z_{R+}\tilde{y}_{s,N}(\omega) - k(1 + \lambda)\tilde{y}_{s,N-1}(\omega) = \sqrt{2}\tilde{\eta}_R(\omega), \tag{17}$$

$$z_{-}\tilde{y}_{a,N}(\omega) - k(1 - \lambda)\tilde{y}_{a,N-1}(\omega) = 0, \tag{18}$$

where  $z_{b+} = -m_0\omega^2 + k_p + 2k(1 + \lambda) - 2\tilde{\Sigma}_b^+(\omega)$ , and  $z_{-} = -m_0\omega^2 + k_p + 2k(1 - \lambda)$  for  $b = L, R$ . Here,  $\tilde{\eta}_b(\omega) = (1/2\pi) \int_{-\infty}^{\infty} dt \eta_b(t)e^{i\omega t}$ . It is also possible to apply the symmetric and anti-symmetric mode transformation first in the time-domain, and then perform the Fourier transforms to these modes. The application of Fourier transforms is only allowed for these modes when they are in steady state. Thus, the aforementioned Eqs. 15 and 17 for the symmetric modes are valid in both the stable and unstable regime as these modes with real frequencies remain bounded at long time even in the unstable regime of the network. However, the Eqs. 16 and 18 are only correct for the network in the stable regime. We can formally write the solution of the symmetric modes as  $\tilde{Y}_s(\omega) = G_s^+(\omega)\tilde{\eta}_s(\omega)$ , where  $\tilde{Y}_s$  and  $\tilde{\eta}_s$  are column vectors of dimension  $N$ :  $\tilde{Y}_s = (\tilde{y}_{s,1}, \tilde{y}_{s,2}, \dots, \tilde{y}_{s,N})^T$  and  $\tilde{\eta}_s = (\sqrt{2}\tilde{\eta}_L, 0, \dots, 0, \sqrt{2}\tilde{\eta}_R)^T$ , and the retarded Green's function  $G_s^+ = Z_s^{-1}/\lambda_+$  with  $\lambda_+ = k(1 + \lambda)$ . Here,  $Z_s$  is a  $N \times N$  symmetric tridiagonal matrix whose offdiagonal elements are  $-1$  and diagonal elements excluding the first and last ones are  $(-m_0\omega^2 + k_p)/\lambda_+ + 2$ . The first and last diagonal elements of  $Z_s$  are  $z_{L+}/\lambda_+$  and  $z_{R+}/\lambda_+$ , respectively.

The steady-state heat current  $\langle J_I \rangle$  after noise averaging over  $J_I(t)$  in Eq. 8 reads

$$\langle J_I \rangle = \int_{-\infty}^{\infty} \frac{d\omega 4\hbar\omega}{\pi} |[G_s^+(\omega)]_{1,N}|^2 \tilde{\Gamma}_L(\omega)\tilde{\Gamma}_R(\omega)(f_L - f_R), \tag{19}$$

where  $\tilde{\Gamma}_b(\omega)$  are the imaginary part of  $\tilde{\Sigma}_b^+(\omega)$ , and  $f_b \equiv f(\omega, T_b) = 1/(e^{\hbar\omega/K_B T_b} - 1)$  is the Bose distribution function for phonons of the left and right ( $b = L, R$ ) heat baths at temperature  $T_b$ . In deriving the current formula, we employ the fluctuation-dissipation relations in the frequency domain:

$$\langle \tilde{\eta}_L(\omega)\tilde{\eta}_L(\omega') \rangle = \frac{\text{Im}[\tilde{\Sigma}_L^+(\omega)]\hbar}{\pi} (1 + f_L)\delta(\omega + \omega'), \tag{20}$$

and a similar relation for the right heat bath. These fluctuation-dissipation relations are true for both these white noise and Rubin baths with an appropriate self-energy contribution. We can derive an explicit expression for the heat current from Eq. 19 in the linear response regime with an applied temperature difference  $\Delta T = T_L - T_R \ll T \equiv (T_L + T_R)/2$ . Expanding the phonon distributions  $f(\omega, T_b)$  about the mean temperature  $T$ , we get

$$\langle J_1 \rangle = \frac{4k_B \Delta T}{\pi} \int_{-2\sqrt{k_0}}^{2\sqrt{k_0}} d\omega \left[ \left( \frac{\hbar\omega}{2k_B T} \right)^2 \operatorname{csch}^2 \left( \frac{\hbar\omega}{2k_B T} \right) \times \tilde{\Gamma}_L(\omega) \tilde{\Gamma}_R(\omega) |[G_s^+(\omega)]_{1,N}|^2 \right]. \tag{21}$$

We can find an analytical expression for heat current in the high-temperature classical regime by taking  $(\hbar\omega/2k_B T)^2 \operatorname{csch}^2(\hbar\omega/2k_B T) \rightarrow 1$ . We get a relatively compact formula of the steady-state classical heat current  $\langle J_1^{cl} \rangle$  by taking  $m_0 = 1, k_p = 0, k(1 + \lambda) = k_0$ , and  $\gamma_L = \gamma_R = \gamma$  for the Rubin baths:

$$\langle J_1^{cl} \rangle = \frac{4k_B \Delta T}{\pi} \int_{-2\sqrt{k_0}}^{2\sqrt{k_0}} d\omega |[G_s^+(\omega)]_{1,N}|^2 \frac{\omega^2 \gamma^4}{k_0^3} \left( 1 - \frac{\omega^2}{4k_0} \right). \tag{22}$$

The required Green’s function element can be found as  $|[G_s^+(\omega)]_{1,N}| = 1/(\lambda + |\det Z_s|)$ . Applying the methods from Refs. [38, 44] for tridiagonal symmetric matrix as explained in detail in Appendix A, we can find a simple form of  $|\det Z_s|$  in the large  $N$  limit with a parametrization  $\omega^2 = 4k_0 \sin^2(q/2)$  to write

$$\begin{aligned} \langle J_1^{cl} \rangle &= \frac{k_B \Delta T \Omega \sqrt{k_0}}{\pi} \int_0^\pi dq \frac{\cos(q/2) \sin^2 q}{\Upsilon - \Omega \cos(2q)} \\ &= \frac{k_B \Delta T \sqrt{k_0}}{\pi} \left( 1 - \sum_{s=\pm 1} \frac{s(\Upsilon - \Omega) \tan^{-1} \left[ \frac{2\sqrt{\Omega}}{\sqrt{-2\Omega + s\sqrt{2\Omega\tilde{\Upsilon}}}} \right]}{2\sqrt{2\tilde{\Upsilon}}\sqrt{-2\Omega + s\sqrt{2\Omega\tilde{\Upsilon}}}} \right), \end{aligned} \tag{23}$$

where  $\Upsilon = k_0^4 - 2k_0^2\gamma^2 + 4\gamma^4$ ,  $\Omega = 2k_0^2\gamma^2$  and  $\tilde{\Upsilon} = \Upsilon + \Omega$ . The system-size independent thermal current is a signature of ballistic heat transport in the harmonic networks of oscillators. The expression in Eq. 23 is valid for different values of  $\lambda$  giving rise to stable and unstable phases.

We also derive an analytical formula of the thermal current in the linear response regime at high temperature for arbitrary  $m_0, k_p, k$ , and  $\lambda$ . We give its derivation in Appendix A. Next, we discuss the features of  $\langle J_1 \rangle$  at low-temperature quantum regime. The  $T$ -dependence of  $\langle J_1 \rangle$  can be extracted from the following expression by considering that only low-frequency (or wavevector) modes contribute in heat current when  $T \rightarrow 0$ . The quantum heat current

$$\begin{aligned} \langle J_1 \rangle &= \frac{k_B \Delta T}{\pi} \int_{-\pi}^\pi dq \left| \frac{d\omega}{dq} \right| |[G_s^+(q)]_{1,N}|^2 \frac{4m_0\omega^2\gamma^4}{k_0^3} \\ &\times \left( 1 - \frac{m_0\omega^2}{4k_0} \right) \left( \frac{\hbar\omega}{2k_B T} \right)^2 \operatorname{csch}^2 \left( \frac{\hbar\omega}{2k_B T} \right), \end{aligned} \tag{24}$$

where  $\omega^2 = (k_p + 4k(1 + \lambda) \sin^2(q/2))/m_0$ . We determine  $T$ -dependence of  $\langle J_1 \rangle$  by finding the leading  $q$ -dependence of  $|[G_s^+(q)]_{1,N}|^2$  in the large  $N$  limit, and performing a scaling analysis of Eq. 24. In the pinned (massive scalar fields) case when  $k_p \neq 0$ , for Rubin baths,



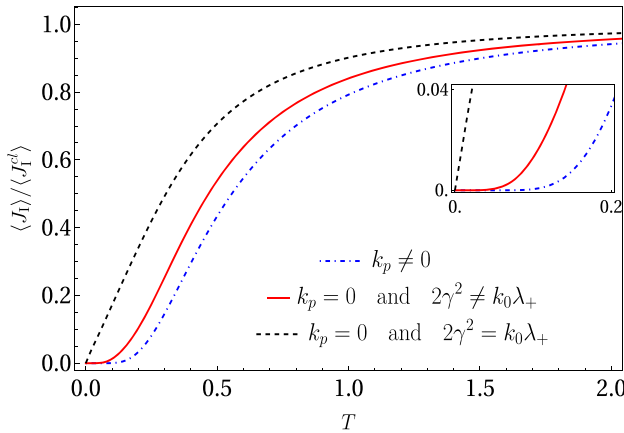


**Fig. 3** Temperature dependence of the scaled heat current  $\langle J_1 \rangle / \langle J_1^{cl} \rangle$  with a single bath at each boundary for different pinning  $k_p$  and bath coupling  $\gamma$ . The inset shows features at low temperature for three different parameter regimes (see text). The temperature is in units of  $(\hbar\sqrt{k}/m_0)/k_B$

we find  $\langle J_1 \rangle \sim (e^{-\hbar\omega_0/(k_B T)})/T^{1/2}$  with  $\omega_0 = \sqrt{k_p/m_0}$  (see Appendix A). For unpinned (massless scalar fields) case when  $k_p = 0$ ,  $\langle J_1 \rangle \sim T^3$  when  $2\gamma^2 \neq k_0\lambda_+$  and  $\langle J_1 \rangle \sim T$  when  $2\gamma^2 = k_0\lambda_+$  as shown in Appendix A. In Fig. 3, we plot the scaled heat current  $\langle J_1 \rangle / \langle J_1^{cl} \rangle$  with temperature when (i)  $k_p/k = 0.5$ ,  $\gamma/k = 0.2$ , (ii)  $k_p = 0$ ,  $\gamma/k = 0.2$  for  $2\gamma^2 \neq k_0\lambda_+$ , and (iii)  $k_p = 0$ ,  $\gamma/k = \sqrt{2.4}$  satisfying  $2\gamma^2 = k_0\lambda_+$ , with  $k_0/k = 4$ ,  $\lambda = 0.2$  and  $m_0 = \hbar = k_B = 1$ . The inset shows the low-temperature features of  $\langle J_1 \rangle / \langle J_1^{cl} \rangle$ . In the numerical analysis, we set  $\Delta T = 0.001$ . The above predicted  $T$ -dependencies of  $\langle J_1 \rangle$  match with the numerical results shown in Fig. 3, for these three different cases.

### 6 Two Baths at Each Boundary

The EOM in Eqs. 9 and 10 for the boundary oscillators connected to two different baths with the same coupling strength read in terms of the symmetric and anti-symmetric modes in the frequency domain as:

$$\tilde{z}_{L+}\tilde{y}_{s,1}(\omega) - k(1 + \lambda)\tilde{y}_{s,2}(\omega) = \tilde{\eta}_{s,L}(\omega), \tag{25}$$

$$\tilde{z}_{L-}\tilde{y}_{a,1}(\omega) - k(1 - \lambda)\tilde{y}_{a,2}(\omega) = \tilde{\eta}_{a,L}(\omega), \tag{26}$$

$$\tilde{z}_{R+}\tilde{y}_{s,N}(\omega) - k(1 + \lambda)\tilde{y}_{s,N-1}(\omega) = \tilde{\eta}_{s,R}(\omega), \tag{27}$$

$$\tilde{z}_{R-}\tilde{y}_{a,N}(\omega) - k(1 - \lambda)\tilde{y}_{a,N-1}(\omega) = \tilde{\eta}_{a,R}(\omega), \tag{28}$$

where  $\tilde{z}_{b\pm} = -m_0\omega^2 + k_p + 2k(1 \pm \lambda) - \tilde{\Sigma}_b^+(\omega)$ ,  $\tilde{\eta}_{s,b}(\omega) = (\tilde{\eta}_{1,b}(\omega) + \tilde{\eta}_{2,b}(\omega))/\sqrt{2}$ , and  $\tilde{\eta}_{a,b}(\omega) = (\tilde{\eta}_{1,b}(\omega) - \tilde{\eta}_{2,b}(\omega))/\sqrt{2}$  for  $b = L, R$ . Similar to the case of single bath at each boundary, the application of Fourier transforms to frequency domain is only allowed for these modes in the steady-state, which occurs for the network in the dynamically stable regime. The EOM for the bulk oscillators in Eq. 12 remain the same for this case. We apply Fourier transformation after switching to these symmetric and anti-symmetric modes. We can again formally write the solution of both the symmetric and anti-symmetric modes as  $\tilde{Y}_{s/a}(\omega) = \tilde{G}_{s/a}^+(\omega)\tilde{\eta}_{s/a}(\omega)$ , where  $\tilde{Y}_{s/a}$  and  $\tilde{\eta}_{s/a}$  are column vectors of dimen-

sion  $N$ :  $\bar{Y}_{s/a} = (\tilde{y}_{s/a,1}, \tilde{y}_{s/a,2}, \dots, \tilde{y}_{s/a,N})^T$  and  $\bar{\eta}_{s/a} = (\tilde{\eta}_{s/a,L}, 0, \dots, 0, \tilde{\eta}_{s/a,R})^T$ , and the retarded Green's functions  $\bar{G}_s^+ = \bar{Z}_s^{-1}/\lambda_+$  and  $\bar{G}_a^+ = \bar{Z}_a^{-1}/\lambda_-$  with  $\lambda_{\pm} = k(1 \pm \lambda)$ . Here,  $\bar{Z}_{s,a}$  are  $N \times N$  symmetric tridiagonal matrices whose offdiagonal elements are  $-1$  and diagonal elements excluding the first and last ones are  $(-m_0\omega^2 + k_p)/\lambda_{+,-} + 2$ . The first and last diagonal elements of  $\bar{Z}_s$  are  $\tilde{z}_{L+}/\lambda_+$  and  $\tilde{z}_{R+}/\lambda_+$ , respectively, and those for  $\bar{Z}_a$  are  $\tilde{z}_{L-}/\lambda_-$  and  $\tilde{z}_{R-}/\lambda_-$ , respectively.

By performing the noise averaging of  $J_{II}$  in Eq. 11, we find the steady-state heat current  $\langle J_{II} \rangle$  in the stable regime of the network as:

$$\langle J_{II} \rangle = \int_{-\infty}^{\infty} d\omega \left[ \frac{\hbar\omega}{\pi} (|[\bar{G}_s^+(\omega)]_{1,N}|^2 + |[\bar{G}_a^+(\omega)]_{1,N}|^2) \times \tilde{\Gamma}_L(\omega)\tilde{\Gamma}_R(\omega)(f_L - f_R) \right], \tag{29}$$

where we have applied the following fluctuation-dissipation relations for the noise averaging:

$$\langle \tilde{\eta}_{\alpha,L}(\omega)\tilde{\eta}_{\beta,L}(\omega') \rangle = \delta_{\alpha,\beta} \frac{\text{Im}[\tilde{\Sigma}_L^+(\omega)]\hbar}{\pi} (1 + f_L)\delta(\omega + \omega'). \tag{30}$$

We again work in the linear response regime for  $\Delta T \ll T$  to derive an analytical expression of  $\langle J_{II} \rangle$ . Expanding the phonon distributions  $f(\omega, T_b)$  about the mean temperature  $T$ , from Eq. 29 we obtain

$$\begin{aligned} \langle J_{II} \rangle &= \frac{k_B \Delta T}{\pi} \left( \int_{-\omega_{1+}}^{\omega_{1+}} d\omega |[\bar{G}_s^+(\omega)]_{1,N}|^2 + \int_{-\omega_{1-}}^{\omega_{1-}} d\omega |[\bar{G}_a^+(\omega)]_{1,N}|^2 \right) \\ &\quad \times \left[ \tilde{\Gamma}_L(\omega)\tilde{\Gamma}_R(\omega) \left( \frac{\hbar\omega}{2k_B T} \right)^2 \text{csch}^2 \left( \frac{\hbar\omega}{2k_B T} \right) \right], \end{aligned} \tag{31}$$

where  $\omega_{1\pm} = \sqrt{(k_p + 4k(1 \pm \lambda))/m_0}$ . In the high-temperature classical regime for the Rubin baths, using Eq. 14, we derive from Eq. 31

$$\langle J_{II}^{cl} \rangle = \frac{k_B \Delta T}{\pi} \left( \int_{-\omega_{1+}}^{\omega_{1+}} d\omega |[\bar{G}_s^+(\omega)]_{1,N}|^2 + \int_{-\omega_{1-}}^{\omega_{1-}} d\omega |[\bar{G}_a^+(\omega)]_{1,N}|^2 \right) \frac{m_0\omega^2\gamma^4}{k_0^3} \left( 1 - \frac{m_0\omega^2}{4k_0} \right). \tag{32}$$

We find the analytical expression of  $[\bar{G}_{s/a}^+(\omega)]_{1,N}$  in the large  $N$  limit following Refs. [38, 44], and then perform the integrals in Eq. 32 to write long analytical formulas for the symmetric and anti-symmetric mode contributions to  $\langle J_{II}^{cl} \rangle$  in Eq. B76 of Appendix B. In addition,  $\langle J_{II}^{cl} \rangle$  is independent of  $N$  indicating ballistic heat transport in the harmonic network for such a bath coupling. We compare  $\langle J_{II}^{cl} \rangle$  to  $\langle J_I^{cl} \rangle$  with increasing  $\lambda$  in the stable regime of the network for similar parameters of the network and the bath coupling strengths  $\gamma$  in Figs. 4, 5. In general,  $\langle J_{II}^{cl} \rangle$  is slightly larger than  $\langle J_I^{cl} \rangle$  for smaller  $\lambda$ s till a specific value of  $\lambda$  (denoted as  $\lambda_a$ ) depending on the value of  $\gamma$  (see Fig. 5). Two baths at each edge facilitate the thermalization of the network better than a single bath at each edge, thus resulting in higher heat transport in the two baths case. We further observe from Eq. B75 that the anti-symmetric mode contribution to  $\langle J_{II}^{cl} \rangle$  vanishes at  $\lambda = 1$ . This is due to the vanishing group velocity of the anti-symmetric modes at  $\lambda = 1$ .

For a given value of  $\gamma$ , we determine the specific coupling strength  $\lambda_a$ , at which  $\langle J_{II}^{cl} \rangle$  exhibits a non-analytic behavior when  $k_p = 0$ . The value of  $\lambda_a$  is obtained analytically by solving the equation  $\gamma^3 + kk_0\gamma(\lambda - 1) = 0$ , which follows from the condition  $\xi_-^a = 1$  (see Eq. B78 in Appendix B), implying  $\lambda_a = 1 - (\gamma^2/kk_0)$ . At  $\lambda_a$ , the analytical expression for the classical current (see Eq. B76 of Appendix B) diverges and  $\langle J_{II}^{cl} \rangle$  is properly defined in the stable regime only upto  $\lambda_a$  as shown in Fig. 5. In other words, the anti-symmetric part of  $\langle J_{II}^{cl} \rangle$  is properly defined only in the regime  $0 < \lambda < \lambda_a$ . Thus, the bath coupling  $\gamma$  reduces

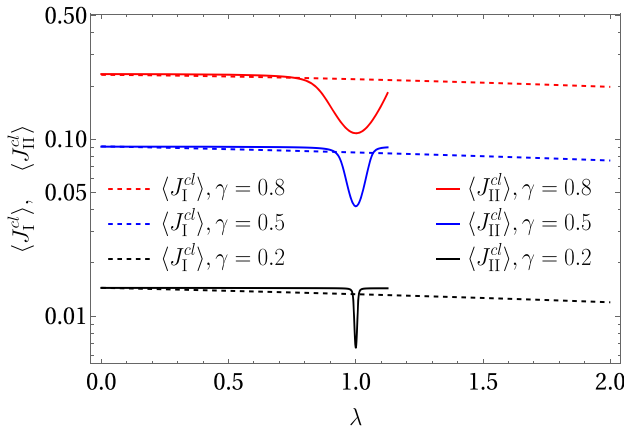


**Fig. 4** Comparison between the high-temperature classical heat currents  $\langle J_I^{cl} \rangle$  (dashed lines) and  $\langle J_{II}^{cl} \rangle$  (solid lines), (the y-axis represents the heat currents multiplied by the common factor  $\pi/(k_B \Delta T)$  in the log scale), with an increasing coupling  $\lambda$  between the fields for different bath coupling strengths  $\gamma$  ( $= 0.8, 0.5, 0.2$  for upper to lower plots). The parameter  $\gamma$  is in units of  $k$ . We set  $k_p = 0.5k, k_0 = 4k$  and  $m_0 = k = \hbar = k_B = 1$  in the numerical analysis. Here,  $\langle J_{II}^{cl} \rangle$  can be defined properly only upto the critical coupling  $\lambda_b \approx 1 + (k_p/4k)$ , which is the large- $N$  limit of  $\lambda_c$

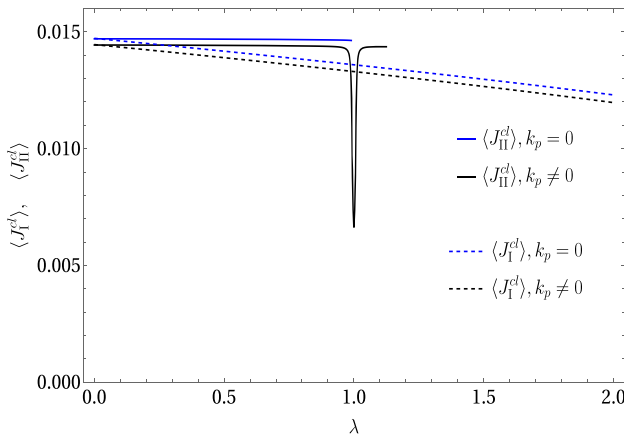


**Fig. 5** Comparison between the high-temperature classical heat currents  $\langle J_I^{cl} \rangle$  (dashed lines) and  $\langle J_{II}^{cl} \rangle$  (solid lines), (the y-axis represents the heat currents multiplied by the common factor  $\pi/(k_B \Delta T)$ ), with an increasing coupling  $\lambda$  between the fields for fixed  $\gamma = 0.2k$  and for both zero and nonzero  $k_p$  values. We set either  $k_p = 0$  (blue) or  $k_p = 0.5k$  (black) and  $k_0 = 4k, m_0 = k = \hbar = k_B = 1$  in the numerical analysis. Here,  $\langle J_{II}^{cl} \rangle$  is again defined properly upto a critical coupling strength  $\lambda_a = 1 - (\gamma^2/kk_0)$  and  $\lambda_b \approx 1 + (k_p/4k)$  for  $k_p = 0$  and  $k_p \neq 0$ , respectively. Notice that the value of current is slightly large for  $k_p = 0$  in both cases

the critical coupling strength of the open network by a factor  $\gamma^2/kk_0$  compared to that of the closed network  $\lambda_c = 1$  (for  $k_p = 0$  and  $N \rightarrow \infty$ ). For  $k_p \neq 0, \langle J_{II}^{cl} \rangle$  does not exhibit any such non-analytic behavior. Nevertheless,  $\langle J_{II}^{cl} \rangle$  falls around  $\lambda_a$  even when  $k_p \neq 0$  due to decreasing contribution of the anti-symmetric modes to  $\langle J_{II}^{cl} \rangle$  with increasing  $\lambda$ .

We finally discuss the features of  $\langle J_{II} \rangle$  at low temperature quantum regime. It can be determined from  $\langle J_{II} \rangle$  in Eq. 31. We could not calculate the integration in Eq. 31 for an

arbitrary temperature. Nevertheless, we can extract  $T$ -dependence of  $\langle J_{\text{II}} \rangle$  by finding leading  $\omega$ -dependence of  $|\overline{G}_{s/a}^+(\omega)|_{1,N}^2$  in the large  $N$  limit, and performing a scaling analysis of Eq. 31. For Rubin baths, we again find in Appendix B,  $\langle J_{\text{II}} \rangle \sim (e^{-\hbar\omega_0/(k_B T)})/T^{1/2}$  with  $\omega_0 = \sqrt{k_p/m_0}$  for pinned (massive scalar fields) case when  $k_p \neq 0$ , which is similar to that for single bath at each boundary and for the white noise baths (see Appendix C). For unpinned (massless scalar fields) case when  $k_p = 0$ ,  $\langle J_{\text{II}} \rangle \sim T$  if either  $\gamma^2 = k_0\lambda_+$  or  $\gamma^2 = k_0\lambda_-$ , and  $\langle J_{\text{II}} \rangle \sim T^3$  when  $\gamma^2 \neq k_0\lambda_+ \neq k_0\lambda_-$  as shown in Appendix B. The corresponding white noise bath cases are discussed in Appendices C and D.

## 7 Summary and Outlook

We have explored heat conduction through a network of different types of oscillators representing a coupled scalar field theory driven by heat baths with different temperatures placed at the boundaries. The dynamical matrix of the network is non-Hermitian and undergoes a stability-to-instability transition at EPs as the coupling strength between the scalar fields (or different types of oscillators) increases. The unstable regime of the dynamical matrix is marked by the emergence of inverted oscillator modes in the network. Consequently, the open network never obtains a steady state in this unstable regime, and the heat current is unbounded for arbitrary bath coupling at the boundaries. In this work, we engineered a unique bath coupling where a single bath is connected to two fields at each edge with the same strength, leading to a finite steady-state heat conduction in the network for any arbitrary coupling strength between the fields. This occurs as the symmetric modes carry the heat, and the heat current is independent of the asymmetric modes, which becomes unbounded in the unstable regime. We also studied the coupling of two fields to two separate baths at each boundary. In this case, heat is carried by both the symmetric and anti-symmetric modes; thus, the heat current is well-behaved only in the stable regime.

We compared heat conduction through the network for collective versus individual coupling of fields to baths at the boundaries. Individual bath coupling of a boundary oscillator is primarily used in studying heat conduction through ordered or disordered networks [41]. We have demonstrated an exciting distinction between different types of bath coupling, and these differences can be significant in the presence of stronger coupling between the network's modes and the baths. In contrast to existing numerical studies in complex networks with multiple modes [32, 41], our explicit analytical formulae in the thermodynamic limit can further aid in understanding the role of various parameters in controlling heat transport in networks with different bath coupling and bath models. One immediate extension of our study could be to explore how heat conduction and the stability-to-instability transition vary due to different types of disorder in the parameters of the network.

Further, we have assumed the fields or oscillator displacements are small for our quadratic modeling of the system Hamiltonian. However, such an assumption breaks down in the unstable regime when the displacement becomes unbounded, and we need to incorporate nonlinear terms in the Hamiltonian [45]. The nonlinear interaction can regularize the heat current in the unstable regime, even for general system-bath couplings [46].

The stability-to-instability transition at the EPs of the non-Hermitian dynamical matrix in our present model is unrelated to a topological phase transition. Nevertheless, recent studies with various quadratic Hermitian bosonic models, whose dynamical matrices resemble non-Hermitian Hamiltonians, have revealed exciting topological phases and phase transitions [21–25]. Investigating heat conduction in such quadratic Hermitian bosonic models could

be applied to identify topological phases and phase transitions in the related non-Hermitian Hamiltonians [47, 48]. Identifying topological phases and phase transitions in non-Hermitian Hamiltonians is a key challenge of significant interest [15, 16, 18, 49, 50]. Studying heat transport in this direction is significant and constitutes one of our future goals.

## Appendix A Single Rubin Bath at Each Boundary

In this appendix, we consider that both types of oscillators at the left or the right end of the network are connected to a single Rubin bath with the same coupling strength. Thus, the couplings between the network and the baths are modeled by the Hamiltonian:

$$H_{c1} = -\gamma_L y_{L,1}(y_{1,1} + y_{2,1}) - \gamma_R y_{R,1}(y_{1,N} + y_{2,N}). \quad (\text{A1})$$

Here,  $y_{L,n}$  and  $y_{R,n}$  represent the left and right bath variables, and  $\gamma_L$  and  $\gamma_R$  are the coupling strengths between the left and right ends of the system and the corresponding baths, respectively. The Rubin baths are modeled as a chain of finite number ( $N_b$ ) of harmonic oscillators with mass  $m_0$  and spring constant  $k_0$  as given by the Hamiltonian:

$$H_b = \sum_{n=1}^{N_b} \frac{p_{b,n}^2}{2m_0} + \sum_{n=0}^{N_b} k_0 \frac{(y_{b,n} - y_{b,n+1})^2}{2}, \quad (\text{A2})$$

with  $b = L, R$ . The total Hamiltonian for the network, two baths and their couplings is  $H_T = H + H_L + H_R + H_{c1}$ . We write the equations of motion (EOM) for the network variables as:

$$m_0 \ddot{y}_{\alpha,n} = -k_p y_{\alpha,n} - k \left[ (2y_{\alpha,n} - y_{\alpha,n-1} - y_{\alpha,n+1}) + \lambda (2y_{\beta,n} - y_{\beta,n+1} - y_{\beta,n-1}) \right] + \gamma_L y_{L,1} \delta_{n,1} + \gamma_R y_{R,1} \delta_{n,N}, \quad (\text{A3})$$

for  $\alpha \neq \beta$ ,  $\alpha, \beta = 1, 2$ ,  $n = 1, 2, \dots, N$  and  $y_{\alpha,0} = y_{\alpha,N+1} = 0$ . The EOM for left and right bath variables are

$$\begin{aligned} m_0 \ddot{y}_{L,1} &= -k_0(2y_{L,1} - y_{L,2}) + \gamma_L(y_{1,1} + y_{2,1}), \\ m_0 \ddot{y}_{R,1} &= -k_0(2y_{R,1} - y_{R,2}) + \gamma_R(y_{1,N} + y_{2,N}), \\ m_0 \ddot{y}_{b,n} &= -k_0(2y_{b,n} - y_{b,n-1} - y_{b,n+1}), \end{aligned} \quad (\text{A4})$$

for  $b = L, R$ ,  $n = 2, 3, \dots, N_b$ . In order to solve the EOM for the bath variables, we rewrite the bath Hamiltonians in Eq. A2 in terms of the normal modes  $Y_{b,r}$ , by using the transformations,  $y_{b,n} = \sum_{r=1}^{N_b} U_{b,nr} Y_{b,r}$  and  $p_{b,n} = \sum_{r=1}^{N_b} U_{b,nr} P_{b,r}$ , where  $U_{b,nr} = (\sqrt{2/(N_b + 1)}) \sin[\pi nr/(N_b + 1)]$ . Thus, we have

$$H_b = \sum_{r=1}^{N_b} \frac{P_{b,r}^2}{2m_0} + \frac{1}{2} m_0 \Omega_{b,r}^2 Y_{b,r}^2, \quad (\text{A5})$$

for  $b = L, R$ , where

$$\Omega_{b,r}^2 = \Omega_r^2 = \frac{4k_0}{m_0} \sin^2 \left( \frac{\pi r}{2(N_b + 1)} \right). \quad (\text{A6})$$

In the last line, we assume  $N_L = N_R$ . Using these normal modes, we rewrite the coupling Hamiltonian in Eq. A1 as:

$$H_{c1} = -\left[\gamma_L(y_{1,1} + y_{2,1}) \sum_{r=1}^{N_L} C_{L,r} Y_{L,r} + \gamma_R(y_{1,N} + y_{2,N}) \sum_{r=1}^{N_R} C_{R,r} Y_{R,r}\right]. \tag{A7}$$

Here,  $C_{b,r} = U_{b,1r}$ . In terms of the aforementioned normal modes, we rewrite the EOM in Eq. A3 as:

$$m_0 \ddot{y}_{\alpha,n} = -k_p y_{\alpha,n} - k \left[ (2y_{\alpha,n} - y_{\alpha,n-1} - y_{\alpha,n+1}) + \lambda(2y_{\beta,n} - y_{\beta,n+1} - y_{\beta,n-1}) \right] + \gamma_L \sum_{r=1}^{N_L} C_{L,r} Y_{L,r} \delta_{n,1} + \gamma_R \sum_{r=1}^{N_R} C_{R,r} Y_{R,r} \delta_{n,N}. \tag{A8}$$

The EOM for the normal modes of baths follow from the Hamiltonians in Eqs. A5 and A7:

$$\begin{aligned} m_0 \ddot{Y}_{L,r} &= -m_0 \Omega_r^2 Y_{L,r} + \gamma_L C_{L,r} (y_{1,1} + y_{2,1}), \\ m_0 \ddot{Y}_{R,r} &= -m_0 \Omega_r^2 Y_{R,r} + \gamma_R C_{R,r} (y_{1,N} + y_{2,N}). \end{aligned} \tag{A9}$$

We solve the above equations for the baths' modes at time  $t > t_0$  with some initial conditions for  $b = L, R$ :

$$Y_{b,r}(t) = f_r^+(t - t_0) Y_{b,r}(t_0) + g_r^+(t - t_0) \dot{Y}_{b,r}(t_0) + \int_{t_0}^t dt' \left[ g_r^+(t - t') \frac{\gamma_b C_{b,r} \sqrt{2}}{m_0} \times (y_{s,1}(t') \delta_{b,L} + y_{s,N}(t') \delta_{b,R}) \right], \tag{A10}$$

where  $f_r^+(t) = \cos(\Omega_r t) \theta(t)$ ,  $g_r^+(t) = \sin(\Omega_r t) \theta(t) / \Omega_r$ , and the symmetric modes  $y_{s,n} = (y_{1,n} + y_{2,n}) / \sqrt{2}$ . Here,  $\theta(t)$  is the Heaviside function. We can further write the EOM for the network variables in Eq. A8 at the boundaries in terms of the symmetric and anti-symmetric modes ( $y_{a,n} = (y_{1,n} - y_{2,n}) / \sqrt{2}$ ) as:

$$\begin{aligned} m_0 \ddot{y}_{s,1} &= -k_p y_{s,1} - k \left[ (2y_{s,1} - y_{s,2}) + \lambda(2y_{s,1} - y_{s,2}) \right] + \sqrt{2} \gamma_L \sum_{r=1}^{N_L} C_{L,r} Y_{L,r}, \\ m_0 \ddot{y}_{s,N} &= -k_p y_{s,N} - k \left[ (2y_{s,N} - y_{s,N-1}) + \lambda(2y_{s,N} - y_{s,N-1}) \right] + \sqrt{2} \gamma_R \sum_{r=1}^{N_R} C_{R,r} Y_{R,r}, \\ m_0 \ddot{y}_{a,1} &= -k_p y_{a,1} - k \left[ (2y_{a,1} - y_{a,2}) - \lambda(2y_{a,1} - y_{a,2}) \right], \\ m_0 \ddot{y}_{a,N} &= -k_p y_{a,N} - k \left[ (2y_{a,N} - y_{a,N-1}) - \lambda(2y_{a,N} - y_{a,N-1}) \right]. \end{aligned} \tag{A11}$$

We notice that the EOM of the anti-symmetric modes do not depend on the bath variables. Nevertheless, they still diverge in time in the inverted oscillator (unstable) regime. Plugging the formal solutions of the left bath variables in Eq. A10 in the EOM for the symmetric modes of the network, we get

$$m_0 \ddot{y}_{s,1} = -k_p y_{s,1} - k(2y_{s,1} - y_{s,2} + \lambda(2y_{s,1} - y_{s,2})) + \int_{t_0}^t dt' \Sigma_L^+(t - t') 2y_{s,1}(t') + \sqrt{2} \eta_L(t). \tag{A12}$$

Here, we identify the operator  $\eta_L(t)$  as a noise from the left bath due to its dependence on the initial condition of the bath variables, and  $\Sigma_L^+(t)$  as a self-energy arising from the coupling of the network to the left bath:

$$\eta_L(t) = \gamma_L \sum_{r=1}^{N_L} C_{L,r} \left( f_r^+(t-t_0) Y_{L,r}(t_0) + g_r^+(t-t_0) \dot{Y}_{L\beta}(t_0) \right), \quad (\text{A13})$$

$$\Sigma_L^+(t) = \sum_{r=1}^{N_L} \frac{\gamma_L^2 C_{L,r}^2}{m_0} g_r^+(t). \quad (\text{A14})$$

Similarly, using the noise and self-energy for the right bath, we obtain:

$$m_0 \ddot{y}_{s,N} = -k_p y_{s,N} - k \left[ (2y_{s,N} - y_{s,N-1}) + \lambda (2y_{s,N} - y_{s,N-1}) \right] + \int_{t_0}^t dt' \Sigma_R^+(t-t') 2y_{s,N}(t') + \sqrt{2} \eta_R(t). \quad (\text{A15})$$

The above equations along with those for the anti-symmetric modes in Eq. A11 are the EOM in Eqs. 6 and 7 in terms of the original system variables after letting  $t_0 \rightarrow -\infty$ . After Fourier transformation to the frequency domain, the EOM in Eqs. A12, A15 and A11 transform into Eqs. 15, 16, 17, and 18.

The self-energy due to bath coupling can be computed as

$$\begin{aligned} \tilde{\Sigma}_b^+(\omega) &= \int_0^\infty \sum_r \frac{\gamma_b^2 C_{b,r}^2}{m_0} \frac{\sin(\Omega_r t)}{\Omega_r} e^{i\omega t} dt \\ &= \lim_{\epsilon \rightarrow 0} \int_0^\infty \sum_r \frac{\gamma_b^2 C_{b,r}^2}{m_0 \Omega_r} \frac{e^{i\Omega_r t} - e^{-i\Omega_r t}}{2i} e^{i\omega t - \epsilon t} dt \\ &= \frac{\gamma_b^2}{k_0} \left[ \left( 1 - \frac{m_0 \omega^2}{2k_0} \right) + i \left( \frac{\sqrt{m_0 \omega}}{\sqrt{k_0}} \left( 1 - \frac{m_0 \omega^2}{4k_0} \right)^{1/2} \right) \right], \end{aligned} \quad (\text{A16})$$

for  $b = L, R$ . The properties of noises are determined by the equilibrium conditions of the isolated baths. Thus,  $\langle \eta_b(t) \rangle = 0$ , and the noise correlation is given by the fluctuation-dissipation relation as

$$\langle \tilde{\eta}_b(\omega) \tilde{\eta}_{b'}(\omega') \rangle = \tilde{\Gamma}_b(\omega) \frac{\hbar}{\pi} (1 + f_b) \delta_{b,b'} \delta(\omega + \omega'), \quad (\text{A17})$$

where  $\tilde{\Gamma}_b(\omega) = \text{Im}(\tilde{\Sigma}_b^+(\omega))$ , and the equilibrium phonon distribution functions  $f_b \equiv f(\omega, T_b) = 1/(e^{\hbar\omega/k_B T_b} - 1)$ , for  $b, b' = L, R$ . Here,  $\langle \dots \rangle$  denotes an expectation over isolated baths' equilibrium distribution.

## A.1 Linear response heat current

We define the heat current at the left boundary of the network as the rate of work done by the left bath on the network, which is given by the expression (see Eq. 8):

$$\begin{aligned} J_1 &= - \left[ \dot{y}_{1,1} \left( \int_{-\infty}^t dt' \Sigma_L^+(t-t') (y_{1,1}(t') + y_{2,1}(t')) + \eta_L \right) \right. \\ &\quad \left. + \dot{y}_{2,1} \left( \int_{-\infty}^t dt' \Sigma_L^+(t-t') (y_{1,1}(t') + y_{2,1}(t')) + \eta_L \right) \right]. \end{aligned} \quad (\text{A18})$$

We express the noise averaged heat current in terms of the symmetric modes in the frequency domain as:

$$\langle J_I \rangle = - \int_{-\infty}^{\infty} d\omega \int_{-\infty}^{\infty} d\omega' e^{-i(\omega+\omega')t} i\omega \left\langle \tilde{y}_{s,1}(\omega) \left( \sqrt{2}\tilde{\eta}_L(\omega') + 2\tilde{\Sigma}_L^+(\omega')\tilde{y}_{s,1}(\omega') \right) \right\rangle. \tag{A19}$$

Here,

$$\tilde{y}_{s,1}(\omega) = [G_s^+(\omega)]_{1,1}\sqrt{2}\tilde{\eta}_L + [G_s^+(\omega)]_{1,N}\sqrt{2}\tilde{\eta}_R, \tag{A20}$$

where,  $G_s^+(\omega)$  is the inverse of the tri-diagonal matrix  $Z$ :

$$Z = \begin{bmatrix} z_{L+} & -\lambda_+ & 0 & \cdots & 0 \\ -\lambda_+ & z_+ & -\lambda_+ & \ddots & \vdots \\ \vdots & \ddots & \ddots & \ddots & \vdots \\ \vdots & & \ddots & \ddots & \vdots \\ \vdots & & & -\lambda_+ & z_+ & -\lambda_+ \\ 0 & \cdots & \cdots & & -\lambda_+ & z_{R+} \end{bmatrix}. \tag{A21}$$

Here,  $z_{b+} = -m_0\omega^2 + k_p + 2\lambda_+ - 2\tilde{\Sigma}_b^+(\omega)$ ,  $z_+ = -m_0\omega^2 + k_p + 2\lambda_+$ , and  $\lambda_+ = k(1 + \lambda)$  for  $b = L, R$ . Thus, we find from Eq. A19:

$$\langle J_I \rangle = - \int_{-\infty}^{\infty} d\omega \int_{-\infty}^{\infty} d\omega' e^{-i(\omega+\omega')t} 2i\omega \times \left\langle \left( [G_s^+(\omega)]_{1,1}\tilde{\eta}_L(\omega) + [G_s^+(\omega)]_{1,N}\tilde{\eta}_R(\omega) \right) \left( \tilde{\eta}_L(\omega') + 2\tilde{\Sigma}_L^+(\omega')([G_s^+(\omega')]_{1,1}\tilde{\eta}_L(\omega') + [G_s^+(\omega')]_{1,N}\tilde{\eta}_R(\omega')) \right) \right\rangle. \tag{A22}$$

The contribution of the right bath to  $\langle J_I \rangle$  in Eq. A22 can be obtained using the fluctuation-dissipation relation for the noise averaging (see Eq. A17) as:

$$\langle J_I^R \rangle = - \int_{-\infty}^{\infty} d\omega \left[ 4|[G_s^+(\omega)]_{1,N}|^2 \tilde{\Gamma}_L(\omega)\tilde{\Gamma}_R(\omega) \frac{\hbar\omega}{\pi} (1 + f_R) \right]. \tag{A23}$$

Similarly, we can find the contribution from the left bath to  $\langle J_I \rangle$  in Eq. A22. We choose  $\tilde{\Gamma}_L(\omega) = \tilde{\Gamma}_R(\omega)$  (which are nonzero only when  $|\omega| < 2\sqrt{k_0}$ ) by setting  $\gamma_L = \gamma_R = \gamma$  to get

$$\langle J_I \rangle = \int_{-2\sqrt{k_0}}^{2\sqrt{k_0}} d\omega \left[ 4|[G_s^+(\omega)]_{1,N}|^2 \frac{m_0\omega^2\gamma^4}{k_0^3} \left( 1 - \frac{m_0\omega^2}{4k_0} \right) \frac{\hbar\omega}{\pi} (f_L - f_R) \right]. \tag{A24}$$

In the linear response regime, after expanding the Bose functions, we get the quantum heat current (see Eq. 24)

$$\langle J_I \rangle = \frac{k_B \Delta T}{\pi} \int_{-2\sqrt{k_0}}^{2\sqrt{k_0}} d\omega \left[ 4|[G_s^+(\omega)]_{1,N}|^2 \frac{m_0\omega^2\gamma^4}{k_0^3} \left( 1 - \frac{m_0\omega^2}{4k_0} \right) \left( \frac{\hbar\omega}{2k_B T} \right)^2 \operatorname{csch}^2 \left( \frac{\hbar\omega}{2k_B T} \right) \right]. \tag{A25}$$

In the high-temperature limit, we obtain the classical heat current in Eq. 22. Next, we find an analytical expression for this classical heat current in the thermodynamic limit.



## A.2 Thermodynamic Limit and an Analytic Expression for Classical Heat Current

To find an analytical expression for the classical current in Eq. 22, we need to manipulate the properties of the matrix  $Z = \lambda_+ Z_s$  in the large  $N$  limit. Given  $N$  number of lattice sites in the network,  $Z_s$  is an  $N \times N$  tridiagonal matrix of the form given in Sect. 5, and we define  $\tilde{a} = (-m_0\omega^2 + k_p)/\lambda_+ + 2$  and  $\epsilon_{L,R} = 2\tilde{\Sigma}_{L,R}^+/\lambda_+$ . We recall that the expression for quantum heat current in Eq. A24 involves the matrix element  $[G_s^+]_{1,N}$ , which is given by the inverse of  $Z$  matrix:  $G_s^+ = Z^{-1} = Z_s^{-1}/\lambda_+$ . From this, we get:

$$|[G_s^+]_{1,N}|^2 = \frac{1}{\lambda_+^2 |\det[Z_s]_N|^2}. \quad (\text{A26})$$

The determinant of a tridiagonal matrix can be obtained through a recursion relation. If all the diagonal entries are  $\tilde{a}$ , then the determinant of an  $N \times N$  matrix is given by the recursion relation:

$$\det([Z_s]_N) = \tilde{a} \det([Z_s]_{N-1}) - \det([Z_s]_{N-2}). \quad (\text{A27})$$

We may simplify the expression for the determinant by assuming  $\tilde{a} = 2 \cos q$ . To simplify this calculation, we further assume  $\omega^2 = 4k_0 \sin^2(q/2)$ , which restricts the following parameters as:  $m_0 = 1$ ,  $k_p = 0$  and  $\lambda_+ = k_0$ . With these simplifications, the determinant takes the form

$$\det[Z_s]_N = \Delta_N = \frac{(A(q) \sin(Nq) + B(q) \cos(Nq))}{\sin q}. \quad (\text{A28})$$

Here,

$$A(q) = -(\epsilon_L + \epsilon_R) + (1 + \epsilon_L \epsilon_R) \cos(q), \quad B(q) = (1 - \epsilon_L \epsilon_R) \sin(q). \quad (\text{A29})$$

From this, we find that

$$|\Delta_N|^2 = \frac{(|A|^2 + |B|^2)(1 + r \sin(2Nq + \phi))}{2 \sin^2 q}, \quad (\text{A30})$$

with  $r \cos \phi = (AB^* + A^*B)/(|A|^2 + |B|^2)$ , and  $r \sin \phi = (|B|^2 - |A|^2)/(|A|^2 + |B|^2)$ .

By substituting  $\omega^2 = 4k_0 \sin^2(q/2)$ , we get the expression for the classical heat current:

$$\langle J_1^{cl} \rangle = \frac{k_B \Delta T}{\pi} \int_{-\pi}^{\pi} dq \left[ |[G_s^+(q)]_{1,N}|^2 \times \sqrt{k_0} \cos\left(\frac{q}{2}\right) \left(\frac{2\gamma^2}{k_0}\right)^2 \sin^2(q) \right]. \quad (\text{A31})$$

For the Rubin baths, we can write the self-energy as  $\tilde{\Sigma}_b^+(q) = (\gamma^2/k_0)e^{iq}$  [see Eq. A16 along with  $\omega^2 = 4k_0 \sin^2(q/2)$ ]. Thus, we can express

$$A(q) = \frac{-4\gamma^2}{k_0^2} \cos q + \left(1 + \frac{4\gamma^4}{k_0^4} \cos 2q\right) \cos q + i \left(\frac{-4\gamma^2}{k_0^2} \sin q + \left(\frac{4\gamma^4}{k_0^4} \sin 2q\right) \cos q\right), \quad (\text{A32})$$

and

$$B(q) = \left(1 - \frac{4\gamma^4}{k_0^4} \cos 2q\right) \sin q - i \frac{4\gamma^4}{k_0^4} \sin 2q \sin q. \quad (\text{A33})$$

Employing the above expressions, we rewrite Eq. A31 as

$$\langle J_1^{cl} \rangle = \frac{k_B \Delta T}{\pi} \int_{-\pi}^{\pi} \frac{dq \sqrt{k_0}}{k_0^2 |\Delta_N|^2} \cos\left(\frac{q}{2}\right) \left(\frac{2\gamma^2}{k_0}\right)^2 \sin^2(q)$$

$$= \frac{k_B \Delta T 16\gamma^4}{\pi k_0^3 \sqrt{k_0}} \int_0^\pi dq \left[ \frac{\cos\left(\frac{q}{2}\right) \sin^4(q)}{(|A|^2 + |B|^2)} \times \frac{1}{(1 + r \sin(2Nq + \phi))} \right]. \tag{A34}$$

In the large  $N$  limit, we can simplify the above integral using the identity [38],

$$\lim_{N \rightarrow \infty} \int_0^\pi dq \frac{g_1(q)}{1 + g_2(q) \sin(Nq)} = \int_0^\pi dq \frac{g_1(q)}{(1 - g_2(q)^2)^{1/2}}, \tag{A35}$$

where, we identify by comparing the above equation with Eq. A34,  $g_2(q) = r$  and

$$g_1(q) = \frac{\cos(q/2) \sin^4(q)}{(|A|^2 + |B|^2)}. \tag{A36}$$

Using  $r$  (see below of Eq. A30 for definitions) and the re-definitions of  $A = a_1 + ia_2$  and  $B = b_1 + ib_2$ , we have

$$(1 - g_2(q))^{1/2} = \frac{2(a_1 b_2 - a_2 b_1)}{|A|^2 + |B|^2}. \tag{A37}$$

Thus, in the large  $N$  limit, the integrand in Eq. A34 simplifies to

$$\int_0^\pi dq \frac{g_1(q)}{(1 - g_2(q))^{1/2}} = \int_0^\pi dq \frac{\cos(q/2) \sin^4 q}{2(|a_1 b_2 - a_2 b_1|)}. \tag{A38}$$

We further derive using  $A(q)$  and  $B(q)$  (see Eq. A29),

$$\begin{aligned} 2(a_1 b_2 - a_2 b_1) &= \frac{8\gamma^2 \sin^2 q (\Upsilon - \Omega \cos(2q))}{k_0^6}, \\ \Upsilon &= k_0^4 - 2k_0^2 \gamma^2 + 4\gamma^4 \quad \text{and} \quad \Omega = 2k_0^2 \gamma^2. \end{aligned} \tag{A39}$$

We thus write the classical heat current as

$$\begin{aligned} \langle J_1^{cl} \rangle &= \frac{k_B \Delta T}{\pi} \frac{2\gamma^2 k_0^3}{\sqrt{k_0}} \int_0^\pi \frac{\cos(q/2) \sin^2 q dq}{\Upsilon - \Omega \cos(2q)} \\ &= \frac{k_B \Delta T \Omega \sqrt{k_0}}{\pi} \int_{-1}^1 dx \frac{\sqrt{\frac{1+x}{2}} \sqrt{1-x^2}}{\Upsilon - \Omega(2x^2 - 1)}, \end{aligned} \tag{A40}$$

where we use the substitution  $x = \cos q$  in the last line. We find Eq. 23 by performing the above integral. Numerical integration of the integral in Eq. A34 (for large  $N$  limit) agrees with the value that obtained directly by numerically inverting the matrix for sufficiently large  $N$ .

### A.3 General Case: Analytical Expression for Classical Current

We may now consider a more general case where we *do not* restrict the parameters as  $m_0 = 1, k_p = 0$  and  $k_0 = \lambda_+$ . We start with the same substitution  $\tilde{a} = 2 \cos q$ . However, now  $\omega^2 \neq 4k_0 \sin^2(q/2)$ , since  $m_0 \neq 1, k_p \neq 0$  and  $k_0 \neq \lambda_+$ . We employ the expression of  $\tilde{\Sigma}^+(\omega)$  in Eq. A16, and the definitions of  $A$  and  $B$  in Eq. A29 to obtain

$$2(a_1 b_2 - a_2 b_1) = \frac{4\gamma^2 \sqrt{(k_p + 4\lambda_+ \sin^2(q/2))(4k_0 - k_p - 4\lambda_+ \sin^2(q/2))}}{k_0^4}$$

$$\times \frac{(4\gamma^4 + k_0^2\lambda_+^2 - 2\lambda_+\gamma^2(\cos q)(2k_0 - k_p - 4\lambda_+ \sin^2(q/2))) \sin q}{\lambda_+^3}. \tag{A41}$$

For a nonzero  $k_p$ , we express the linear response classical heat current as:

$$\langle J_I^{cl} \rangle = \frac{k_B \Delta T}{\pi} \int_{-\omega_{1+}}^{\omega_{1+}} d\omega |[G_s^+(\omega)]_{1,N}|^2 \times \frac{4m_0\omega^2\gamma^4}{k_0^3} \left(1 - \frac{m_0\omega^2}{4k_0}\right), \tag{A42}$$

where  $\omega_{1+} = \sqrt{(k_p + 4\lambda_+)/m_0}$ . Substituting  $\omega^2 = (k_p + 4\lambda_+ \sin^2(q/2))/m_0$  in the above expression, we get

$$\langle J_I^{cl} \rangle = \frac{k_B \Delta T}{\pi} \int_{-\pi}^{\pi} dq \left[ \left| \frac{d\omega}{dq} \right| |[G_s^+(\omega)]_{1,N}|^2 \times \frac{4m_0\omega^2\gamma^4}{k_0^3} \left(1 - \frac{m_0\omega^2}{4k_0}\right) \right]. \tag{A43}$$

where,  $|d\omega/dq| = (\lambda_+ \sin q)/(m_0\omega)$ . Applying the expression for  $\Delta_N$  in the large  $N$  limit (as in Eq. A35), we re-express the above current as

$$\langle J_I^{cl} \rangle = \frac{k_B \Delta T}{\pi} \int_0^{\pi} dq \frac{(\sin^2 q)\gamma^2\lambda_+^2\sqrt{4k_0 - k_p - 4\lambda_+ \sin^2(q/2)}}{\sqrt{m_0}(4\gamma^4 + k_0^2\lambda_+^2 - 2\gamma^2\lambda_+(\cos q)(2k_0 - k_p - 4\lambda_+ \sin^2(q/2)))}, \tag{A44}$$

where we use Eq. A41 along with the form of Eq. A37. We substitute  $x = \cos q$  to get

$$\langle J_I^{cl} \rangle = \frac{k_B \Delta T}{\pi\sqrt{m_0}} \int_{-1}^1 \frac{dx \gamma^2\lambda_+^2\sqrt{1-x^2}\sqrt{4k_0 - k_p - 2\lambda_+(1-x)}}{4\gamma^4 + k_0^2\lambda_+^2 - 2\gamma^2\lambda_+x(2k_0 - k_p - 2\lambda_+(1-x))}. \tag{A45}$$

The above definite integral can be expressed in terms of complete and incomplete elliptic integrals of first ( $K$  and  $F$ ), second ( $E$ ) and third kind ( $\Pi$ ). Thus, we obtain

$$\begin{aligned} \langle J_I^{cl} \rangle &= \frac{k_B \Delta T}{4\pi\sqrt{m_0}\sqrt{k_p - 4k_0 + 4\lambda_+}} [-2(k_p + 4\lambda_+ - 4k_0)(E(\phi, \zeta) + E(\zeta)) \\ &\quad + 4(\lambda_+ - k_0)(F(\phi, \zeta) + K(\zeta)) \\ &\quad + (k_p + 2\lambda_+ - 2k_0)(\Pi(\xi_-, \phi, \zeta) + \Pi(\xi_+, \phi, \zeta) + \Pi(\xi_-, \zeta) + \Pi(\xi_+, \zeta)) \\ &\quad + \frac{\gamma^2(4k_0^2 - 4k_0(k_p + 2\lambda_+) + k_p^2 + 4k_p\lambda_+ - 4\lambda_+^2) + 2k_0^2\lambda_+^2 + 8\gamma^4}{\sqrt{4\gamma^2k_0^2\lambda_+^2 + \gamma^4(-2k_0 + k_p + 2\lambda_+)^2 + 16\gamma^6}} \\ &\quad \times (\Pi(\xi_-, \phi, \zeta) - \Pi(\xi_+, \phi, \zeta) + \Pi(\xi_-, \zeta) - \Pi(\xi_+, \zeta))], \end{aligned} \tag{A46}$$

where

$$\begin{aligned} \phi &= i \sinh^{-1} \left( \sqrt{\frac{4k_0 - k_p - 4\lambda_+}{k_p - 4k_0}} \right), \quad \zeta = \frac{k_p - 4k_0}{k_p + 4\lambda_+ - 4k_0}, \\ \xi_{\pm} &= \frac{2\gamma^2(k_p - 4k_0)}{\gamma^2(-6k_0 + k_p + 2\lambda_+) \pm \sqrt{2\Omega\lambda_+^2 + \gamma^4(-2k_0 + k_p + 2\lambda_+)^2 + 16\gamma^6}}. \end{aligned} \tag{A47}$$

### A.4 Temperature Dependence of Low-Temperature $\langle J_I \rangle$

Here, we determine the temperature dependence of the low-temperature heat current  $\langle J_I \rangle$ . The quantum current  $\langle J_I \rangle$  in the linear response regime reads from Eq. A25 as:

$$\langle J_I \rangle = \frac{4k_B \Delta T}{\pi} \int_{-\pi}^{\pi} dq \left[ \left| \frac{d\omega}{dq} \right| | [G_s^+(q)]_{1,N} |^2 \frac{m_0 \omega^2 \gamma^4}{k_0^3} \times \left( 1 - \frac{m_0 \omega^2}{4k_0} \right) \left( \frac{\hbar \omega}{2k_B T} \right)^2 \operatorname{csch}^2 \left( \frac{\hbar \omega}{2k_B T} \right) \right], \tag{A48}$$

where  $\omega^2 = (k_p + 4\lambda_+ \sin^2(q/2))/m_0$ . Since the low-frequency or low-wavevector modes mostly contribute in heat conduction at low temperature, we determine the temperature dependence of low-temperature  $\langle J_I \rangle$  by studying the above integrand in the limit of small  $\omega$  or  $q$ . We rewrite the integrand in Eq. A48 in the large  $N$  limit in terms of the system parameters as:

$$\langle J_I \rangle = \frac{\hbar^2 \Delta T}{4\pi k_B \sqrt{m_0} T^2} \int_0^{\pi} dq \left[ \frac{\gamma^2 \lambda_+^2 \sin^2(q) \sqrt{4k_0 - m_0 \omega^2}}{\Lambda - 2\gamma^2 \lambda_+ \cos(q) (2k_0 - m_0 \omega^2)} \omega^2 \operatorname{csch}^2 \left( \frac{\hbar \omega}{2k_B T} \right) \right], \tag{A49}$$

where,  $\Lambda = (4\gamma^4 + k_0^2 \lambda_+^2)$ . We take the limit of small  $q$  for  $k_p \neq 0$  to find:

$$\langle J_I \rangle \approx \frac{\hbar^2 \Delta T}{\pi k_B \sqrt{m_0} T^2} e^{-\frac{\hbar \omega_0}{k_B T}} \int_0^{\pi} dq \left[ \frac{\gamma^2 \lambda_+^2 q^2 \sqrt{4k_0 - k_p - \lambda_+ q^2}}{(\Lambda - 2\gamma^2 \lambda_+ (1 - q^2/2) (2k_0 - k_p - \lambda_+ q^2))} \times \left( \frac{k_p}{m_0} + \frac{\lambda_+ q^2}{m_0} \right) e^{-\frac{\hbar \lambda_+ q^2}{2k_B T m_0 \omega_0}} \right], \tag{A50}$$

where we approximate  $\omega^2 \approx (k_p + \lambda_+ q^2)/m_0$  and  $\operatorname{csch}^2 [\hbar \omega / (2k_B T)] \approx 4e^{-\hbar \omega_0 / (k_B T)} e^{-\hbar \lambda_+ q^2 / (2k_B T m_0 \omega_0)}$ . By substituting  $x = (\hbar \lambda_+ q^2) / (2k_B T m_0 \omega_0)$ , we obtain the leading-order  $T$ -dependence of  $\langle J_I \rangle$  for  $k_p \neq 0$  as:

$$\langle J_I \rangle \sim \frac{e^{-\frac{\hbar \omega_0}{k_B T}}}{\sqrt{T}} \quad \text{with} \quad \omega_0 = \sqrt{\frac{k_p}{m_0}}. \tag{A51}$$

For  $k_p = 0$ , we notice that  $\omega \propto q$  for small  $q$ . We substitute  $x = (\hbar \omega) / (2k_B T)$  in Eq. A49. Moreover, the denominator of the integrand in Eq. A49 can be re-expressed in the small  $q$  limit as

$$(2\gamma^2 - k_0 \lambda_+)^2 + (2k_0 \lambda_+ \gamma^2 + 2\gamma^2 \lambda_+^2) q^2. \tag{A52}$$

Thus, analytically, we get  $\langle J_I \rangle \sim T$ , when  $2\gamma^2 = k_0 \lambda_+$  and  $\langle J_I \rangle \sim T^3$  when  $2\gamma^2 \neq k_0 \lambda_+$ . We verified these results numerically.

### Appendix B Two Rubin Baths at Each Boundary

In this appendix, we consider the case where two types of oscillators at the left and right end of the network are connected to two different Rubin baths. Thus, the network-bath coupling is given by the Hamiltonian:

$$H_{c2} = -\gamma_L^{(1)} y_{L,1}^{(1)} y_{1,1} - \gamma_L^{(2)} y_{L,1}^{(2)} y_{2,1} - \gamma_R^{(1)} y_{R,1}^{(1)} y_{1,N} - \gamma_R^{(2)} y_{R,1}^{(2)} y_{2,N}. \tag{B53}$$

Here,  $y_{L,n}^{(1)/(2)}$  represent two different types of left bath variables (differentiated by the superscripts (1) and (2)), and  $y_{R,n}^{(1)/(2)}$  represent those for the right baths. Moreover,  $\gamma_L^{(1)/(2)}$  and  $\gamma_R^{(1)/(2)}$  are the coupling strengths between the left and right ends of the network and the corresponding baths, respectively. The total Hamiltonian for the network and four baths including the coupling is  $H_T = H + H_L^{(1)} + H_L^{(2)} + H_R^{(1)} + H_R^{(2)} + H_{c2}$ . Here,  $H_b^{(1)/(2)}$  (for  $b = L, R$ ) are the Hamiltonians of two types of Rubin baths at each end, as defined in Eq. A2 of Appendix A. At first, we write down the EOM for the network variables in terms of the normal modes of the bath variables (see Eq. A5) as:

$$\begin{aligned}
 m_0 \ddot{y}_{\alpha,n} = & -k_p y_{\alpha,n} - k \left[ (2y_{\alpha,n} - y_{\alpha,n-1} - y_{\alpha,n+1}) + \lambda(2y_{\beta,n} - y_{\beta,n+1} - y_{\beta,n-1}) \right] \\
 & + \gamma_L^{(1)} \sum_{r=1}^{N_L} C_{L,r} Y_{L,r}^{(1)} \delta_{n,1} \delta_{\alpha,1} + \gamma_R^{(1)} \sum_{r=1}^{N_R} C_{R,r} Y_{R,r}^{(1)} \delta_{n,N} \delta_{\alpha,N} \\
 & + \gamma_L^{(2)} \sum_{r=1}^{N_L} C_{L,r} Y_{L,r}^{(2)} \delta_{n,1} \delta_{\alpha,2} + \gamma_R^{(2)} \sum_{r=1}^{N_R} C_{R,r} Y_{R,r}^{(2)} \delta_{n,N} \delta_{\alpha,2},
 \end{aligned} \tag{B54}$$

for  $\alpha \neq \beta, \alpha, \beta = 1, 2, n = 1, 2, \dots, N$  and  $y_{\alpha,0} = y_{\alpha,N+1} = 0$ . Here,  $y_{b,n}^{(1)/(2)} = \sum_{r=1}^{N_b} U_{b,nr} Y_{b,r}^{(1)/(2)}$  and  $C_{b,r} = U_{b,1r}$  for  $b = L, R$  (see Appendix A for details). Similarly, we obtain the EOM for the bath variables:

$$\begin{aligned}
 m_0 \ddot{Y}_{L,r}^{(1)/(2)} = & -m_0 \Omega_{L,r}^2 Y_{L,r}^{(1)/(2)} + \gamma_L^{(1)/(2)} C_{L,r} y_{1/2,1}, \\
 m_0 \ddot{Y}_{R,r}^{(1)/(2)} = & -m_0 \Omega_{R,r}^2 Y_{R,r}^{(1)/(2)} + \gamma_R^{(1)/(2)} C_{R,r} y_{1/2,N}.
 \end{aligned} \tag{B55}$$

Here,  $\Omega_{b,r}^2 = \Omega_r^2 = (4k_0/m_0) \sin^2 [\pi r / (2(N_b + 1))]$  are the normal frequencies assuming  $N_L = N_R$ . Consequently, the formal solutions at  $t > t_0$  are:

$$\begin{aligned}
 Y_{b,r}^{(1)/(2)}(t) = & f_r^+(t - t_0) Y_{b,r}^{(1)/(2)}(t_0) + g_r^+(t - t_0) \dot{Y}_{b,r}^{(1)/(2)}(t_0) \\
 & + \int_{t_0}^t dt' \left[ g_r^+(t - t') \frac{\gamma_b^{(1)/(2)} C_{b,r}}{m_0} \times (y_{1/2,1}(t') \delta_{b,L} + y_{1/2,N}(t') \delta_{b,R}) \right],
 \end{aligned} \tag{B56}$$

where  $f_r^+(t) = \cos(\Omega_r t) \theta(t)$ ,  $g_r^+(t) = \sin(\Omega_r t) \theta(t) / \Omega_r$ . Substituting these formal solutions in Eq. B54 for the boundary variables imply Eqs. 9 and 10 after letting  $t_0 \rightarrow -\infty$ , provided we identify the noises  $\eta_{1/2,L}(t)$  and self-energies  $\Sigma_{1/2,L}^+(t)$  as:

$$\eta_{1/2,L}(t) = \gamma_L^{(1)/(2)} \sum_{r=1}^{N_L} C_{L,r} \left( f_r^+(t - t_0) Y_{L,r}^{(1)/(2)}(t_0) + g_r^+(t - t_0) \dot{Y}_{L,r}^{(1)/(2)}(t_0) \right), \tag{B57}$$

and

$$\Sigma_{1/2,L}^+(t) = \sum_{r=1}^{N_L} \frac{\left( \gamma_L^{(1)/(2)} \right)^2 C_{L,r}^2}{m_0} g_r^+(t). \tag{B58}$$

Similar definitions hold for the noises  $\eta_{1/2,R}(t)$  and self-energies  $\Sigma_{1/2,R}^+(t)$  of the right baths. Now, we rewrite these equations (assuming same coupling strengths  $\gamma_b^{(1)} = \gamma_b^{(2)}$ , which implies  $\Sigma_{1,b}^+ = \Sigma_{2,b}^+ = \Sigma_b^+$  for  $b = L, R$ ) in terms of the symmetric and anti-symmetric variables as:

$$\begin{aligned}
 m_0 \ddot{y}_{s,1} &= -k_p y_{s,1} - k[2y_{s,1} - y_{s,2} + \lambda(2y_{s,1} - y_{s,2})] \\
 &+ \int_{t_0}^t dt' \Sigma_L^+(t-t') y_{s,1}(t') + \eta_{s,L},
 \end{aligned} \tag{B59}$$

$$\begin{aligned}
 m_0 \ddot{y}_{s,N} &= -k_p y_{s,N} - k[2y_{s,N} - y_{s,N-1} + \lambda(2y_{s,N} - y_{s,N-1})] \\
 &+ \int_{t_0}^t dt' \Sigma_R^+(t-t') y_{s,N}(t') + \eta_{s,R}.
 \end{aligned} \tag{B60}$$

Here,  $\eta_{s/a,L} = (\eta_{1,L}(t) \pm \eta_{2,L}(t))/\sqrt{2}$ . Similarly, for the anti-symmetric variables, we get

$$\begin{aligned}
 m_0 \ddot{y}_{a,1} &= -k_p y_{a,1} - k[2y_{a,1} - y_{a,2} - \lambda(2y_{a,1} - y_{a,2})] \\
 &+ \int_{t_0}^t dt' \Sigma_L^+(t-t') y_{a,1}(t') + \eta_{a,L},
 \end{aligned} \tag{B61}$$

$$\begin{aligned}
 m_0 \ddot{y}_{a,N} &= -k_p y_{a,N} - k[2y_{a,N} - y_{a,N-1} - \lambda(2y_{a,N} - y_{a,N-1})] \\
 &+ \int_{t_0}^t dt' \Sigma_R^+(t-t') y_{a,N}(t') + \eta_{a,R}.
 \end{aligned} \tag{B62}$$

We notice that, letting  $t_0 \rightarrow -\infty$  and taking a Fourier transformation to the frequency domain, the above EOM in Eqs. B59, B60, B61, and B62 transform into Eqs. 25, 27, 26, and 28, respectively.

### B.1 Linear Response Heat Current

We define the heat current at the left boundary of the network as the rate of work done by the baths, which is given by the expression in Eq. 11. It can be re-expressed in terms of symmetric and anti-symmetric variables as

$$\begin{aligned}
 J_{\Pi} &= -\left[ \dot{y}_{s,1} \eta_{s,L} + \dot{y}_{a,1} \eta_{a,L} + \left( \frac{\dot{y}_{s,1} + \dot{y}_{a,1}}{\sqrt{2}} \right) \int_{-\infty}^t dt' \Sigma_L^+(t-t') \left( \frac{y_{s,1} + y_{a,1}}{\sqrt{2}} \right) \right. \\
 &\left. + \left( \frac{\dot{y}_{s,1} - \dot{y}_{a,1}}{\sqrt{2}} \right) \int_{-\infty}^t dt' \Sigma_L^+(t-t') \left( \frac{y_{s,1} - y_{a,1}}{\sqrt{2}} \right) \right].
 \end{aligned} \tag{B63}$$

Now going into the Fourier modes in the frequency domain, we have the noise averaged heat current:

$$\begin{aligned}
 \langle J_{\Pi} \rangle &= -\int_{-\infty}^{\infty} d\omega \int_{-\infty}^{\infty} d\omega' e^{-i(\omega+\omega')t} \left\{ i\omega \tilde{y}_{s,1}(\omega) \tilde{\eta}_{s,L}(\omega') + i\omega \tilde{\Sigma}_L^+(\omega') \tilde{y}_{s,1}(\omega) \tilde{y}_{s,1}(\omega') \right. \\
 &\left. + i\omega \tilde{y}_{a,1}(\omega) \tilde{\eta}_{a,L}(\omega') + i\omega \tilde{\Sigma}_L^+(\omega') \tilde{y}_{a,1}(\omega) \tilde{y}_{a,1}(\omega') \right\}.
 \end{aligned} \tag{B64}$$

From Eqs. 25, 26, 27, and 28, we notice that

$$\begin{aligned}
 \tilde{y}_{s,1} &= [\bar{G}_s^+]_{1,1} \left( \frac{\tilde{\eta}_{1,L} + \tilde{\eta}_{2,L}}{\sqrt{2}} \right) + [\bar{G}_s^+]_{1,N} \left( \frac{\tilde{\eta}_{1,R} + \tilde{\eta}_{2,R}}{\sqrt{2}} \right), \\
 \tilde{y}_{a,1} &= [\bar{G}_a^+]_{1,1} \left( \frac{\tilde{\eta}_{1,L} - \tilde{\eta}_{2,L}}{\sqrt{2}} \right) + [\bar{G}_a^+]_{1,N} \left( \frac{\tilde{\eta}_{1,R} - \tilde{\eta}_{2,R}}{\sqrt{2}} \right).
 \end{aligned} \tag{B65}$$

Here,  $\bar{G}_{s/a}^+$  are the inverses of the matrices  $\tilde{Z}^{s/a}$ , defined as

$$\tilde{Z}^{s/a} = \begin{bmatrix} \tilde{z}_{L\pm} & -\lambda_{\pm} & 0 & \cdots & & 0 \\ -\lambda_{\pm} & \tilde{z}_{\pm} & -\lambda_{\pm} & \ddots & & \vdots \\ \vdots & \ddots & \ddots & \ddots & \ddots & \vdots \\ \vdots & & \ddots & \ddots & \ddots & \vdots \\ \vdots & & & -\lambda_{\pm} & \tilde{z}_{\pm} & -\lambda_{\pm} \\ 0 & \cdots & \cdots & & -\lambda_{\pm} & \tilde{z}_{R\pm} \end{bmatrix}, \quad (\text{B66})$$

where,  $\tilde{z}_{b\pm} = -m_0\omega^2 + k_p + 2\lambda_{\pm} - \tilde{\Sigma}_b^+(\omega)$ ,  $\tilde{z}_{\pm} = -m_0\omega^2 + k_p + 2\lambda_{\pm}$  and  $\lambda_{\pm} = k(1 \pm \lambda)$  for  $b = L, R$ . Notice that here,  $\lambda_+$  and  $\lambda_-$  correspond to  $\tilde{Z}^s$  and  $\tilde{Z}^a$ , respectively. Now using the fluctuation-dissipation relation (see also Eq. (A17) in Appendix A),

$$\langle \tilde{\eta}_{a,b}(\omega) \tilde{\eta}_{a',b'}(\omega') \rangle = \frac{\tilde{\Gamma}_b(\omega) \hbar}{\pi} (1 + f_b) \delta_{b,b'} \delta_{a,a'} \delta(\omega + \omega'), \quad (\text{B67})$$

where  $a, a' = 1, 2$ , for noise averaging to get the right-part of the heat current as

$$\langle J_{\text{II}}^R \rangle = - \int_{-\infty}^{\infty} d\omega \left[ (|\tilde{G}_s^+(\omega)|_{1,N}|^2 + |\tilde{G}_a^+(\omega)|_{1,N}|^2) \times \tilde{\Gamma}_L(\omega) \tilde{\Gamma}_R(\omega) \frac{\hbar\omega}{\pi} (1 + f_R) \right]. \quad (\text{B68})$$

Similarly, finding the contribution from the left baths implies the expression for the total current as in Eq. 29. Now, we choose  $\tilde{\Gamma}_L(\omega) = \tilde{\Gamma}_R(\omega)$  (which are nonzero only when  $|\omega| < 2\sqrt{k_0}$ ) by setting  $\gamma_L^{(1)/(2)} = \gamma_R^{(1)/(2)} = \gamma$  to get

$$\langle J_{\text{II}} \rangle = \int_{-2\sqrt{k_0}}^{2\sqrt{k_0}} d\omega \left[ (|\tilde{G}_s^+(\omega)|_{1,N}|^2 + |\tilde{G}_a^+(\omega)|_{1,N}|^2) \frac{m_0\omega^2\gamma^4}{k_0^3} \left( 1 - \frac{m_0\omega^2}{4k_0} \right) \frac{\hbar\omega}{\pi} (f_L - f_R) \right]. \quad (\text{B69})$$

In the linear response regime, we have

$$\langle J_{\text{II}} \rangle = \frac{k_B \Delta T}{\pi} \int_{-2\sqrt{k_0}}^{2\sqrt{k_0}} d\omega \left[ (|\tilde{G}_s^+(\omega)|_{1,N}|^2 + |\tilde{G}_a^+(\omega)|_{1,N}|^2) \frac{m_0\omega^2\gamma^4}{k_0^3} \left( 1 - \frac{m_0\omega^2}{4k_0} \right) \times \left( \frac{\hbar\omega}{2k_B T} \right)^2 \text{csch}^2 \left( \frac{\hbar\omega}{2k_B T} \right) \right]. \quad (\text{B70})$$

Next, we obtain an analytical expression for the classical current in the thermodynamic limit.

## B.2 Thermodynamic Limit and an Analytic Expression for the classical Current

To find an analytical expression for the classical current, we manipulate the properties of the matrices  $\tilde{Z}^{s/a} = \lambda_{\pm} \cdot \bar{Z}_{s/a}$  in the large  $N$  limit. Given  $N$  number of lattice sites in the network,  $\bar{Z}_{s/a}$  matrices are  $N \times N$  tridiagonal matrices of the form given in Sect. 6. Now, we define  $\tilde{a}_{\pm} = ((-m_0\omega^2 + k_p)/\lambda_{\pm}) + 2$  and  $\epsilon_{L,R} = \tilde{\Sigma}_{L,R}^+/\lambda_{\pm}$  for  $\bar{Z}_s$  and  $\bar{Z}_a$ , respectively. Since these are tridiagonal matrices, we obtain

$$|\tilde{G}_{s/a}^+|_{1,N}|^2 = \frac{1}{(\lambda_{\pm})^2 |\det[\bar{Z}_{s/a}]_N|^2}. \quad (\text{B71})$$

We simplify the expression for determinant by assuming  $\tilde{a}_{\pm} = 2 \cos q$ . This implies  $m_0 \omega_{s/a}^2 = k_p + 4\lambda_{\pm} \sin^2(q/2)$  for  $\bar{Z}_s$  and  $\bar{Z}_a$ , respectively. As explained in Appendix A, we find the determinant of the matrices  $\bar{Z}_{s/a}$  in the large  $N$  limit (see Eqs. A28, A29, and A30). In this case, from the matrix elements of  $\bar{Z}_s$  and  $\bar{Z}_a$  along with Eqs. A16 and A29, we get  $(\lambda_{\pm})$  correspond to  $\bar{Z}_s$  and  $\bar{Z}_a$ , respectively):

$$2(a_1 b_2 - a_2 b_1) = \frac{2\gamma^2 \sqrt{(k_p + 4\lambda_{\pm} \sin^2(q/2))(4k_0 - k_p - 4\lambda_{\pm} \sin^2(q/2))}}{k_0^4} \times \frac{(\gamma^4 + k_0^2 \lambda_{\pm}^2 - \lambda_{\pm} \gamma^2 (\cos q)(2k_0 - k_p - 4\lambda_{\pm} \sin^2(q/2))) \sin q}{\lambda_{\pm}^3}. \tag{B72}$$

Here, the classical current can be expressed as in Eq. 32 in the linear response regime. We use the expression for  $\Delta_N$  (see Eq. A28) in the large  $N$  limit to re-express the symmetric and anti-symmetric parts of the current as

$$\langle J_{II}^{cl} \rangle^{s/a} = \frac{k_B \Delta T}{\pi} \int_0^{\pi} dq \frac{g_1^{s/a}(q)}{(1 - g_2^{s/a}(q)^2)^{1/2}}. \tag{B73}$$

Now, we use the form of Eqs. A37 and B72 to simplify the integrand in the expression for classical current (where we define  $\Lambda_{\pm} = \gamma^4 + k_0^2 \lambda_{\pm}^2$ ) as:

$$\frac{g_1^{s/a}(q)}{(1 - g_2^{s/a}(q)^2)^{1/2}} = \frac{(\sin^2 q) \gamma^2 \lambda_{\pm}^2 \sqrt{4k_0 - k_p - 4\lambda_{\pm} \sin^2(q/2)}}{2\sqrt{m_0} (\Lambda_{\pm} - \gamma^2 \lambda_{\pm} (\cos q)(2k_0 - k_p - 4\lambda_{\pm} \sin^2(q/2)))}. \tag{B74}$$

The substitution  $x = \cos q$  simplifies the symmetric and anti-symmetric parts of the classical current:

$$\langle J_{II}^{cl} \rangle^{s/a} = \frac{k_B \Delta T}{2\pi \sqrt{m_0}} \int_{-1}^1 \frac{dx \gamma^2 \lambda_{\pm}^2 \sqrt{1 - x^2} \sqrt{4k_0 - k_p - 2\lambda_{\pm}(1 - x)}}{\Lambda_{\pm} - \gamma^2 \lambda_{\pm} x (2k_0 - k_p - 2\lambda_{\pm}(1 - x))}. \tag{B75}$$

We may evaluate this integral in terms of elliptic integrals as in the previous case to obtain (for  $0 \leq \lambda < 1$ )

$$\begin{aligned} \langle J_{II}^{cl} \rangle^{s/a} &= \frac{k_B \Delta T}{4\pi \sqrt{m_0} \sqrt{k_p - 4k_0 + 4\lambda_{\pm}}} \left[ -2(k_p + 4\lambda_{\pm} - 4k_0)(E(\phi^{s/a}, \zeta^{s/a}) + E(\zeta^{s/a})) \right. \\ &\quad + 4(\lambda_{\pm} - k_0)(F(\phi^{s/a}, \zeta^{s/a}) + K(\zeta^{s/a})) \\ &\quad + (k_p + 2\lambda_{\pm} - 2k_0) \left( \Pi(\xi_{-}^{s/a}, \phi^{s/a}, \zeta^{s/a}) + \Pi(\xi_{+}^{s/a}, \phi^{s/a}, \zeta^{s/a}) \right. \\ &\quad \left. + \Pi(\xi_{-}^{s/a}, \zeta^{s/a}) + \Pi(\xi_{+}^{s/a}, \zeta^{s/a}) \right) \\ &\quad + \frac{\gamma^2 \left( 4k_0^2 - 4k_0(k_p + 2\lambda_{\pm}) + k_p^2 + 4k_p \lambda_{\pm} - 4\lambda_{\pm}^2 \right) + 4k_0^2 \lambda_{\pm}^2 + 4\gamma^4}{\sqrt{8\gamma^2 k_0^2 \lambda_{\pm}^2 + \gamma^4 (-2k_0 + k_p + 2\lambda_{\pm})^2 + 8\gamma^6}} \\ &\quad \times \left( \Pi(\xi_{-}^{s/a}, \phi^{s/a}, \zeta^{s/a}) - \Pi(\xi_{+}^{s/a}, \phi^{s/a}, \zeta^{s/a}) \right) \\ &\quad \left. + \Pi(\xi_{-}^{s/a}, \zeta^{s/a}) - \Pi(\xi_{+}^{s/a}, \zeta^{s/a}) \right]. \tag{B76} \end{aligned}$$



Here,  $\lambda_{\pm}$  correspond to  $\langle J_{\Pi}^{cl} \rangle^{s/a}$ , respectively, and

$$\phi^{s/a} = i \sinh^{-1} \left( \sqrt{\frac{4k_0 - k_p - 4\lambda_{\pm}}{k_p - 4k_0}} \right), \quad \zeta^{s/a} = \frac{k_p - 4k_0}{k_p + 4\lambda_{\pm} - 4k_0} \tag{B77}$$

and

$$\xi_{\pm}^{s/a} = \frac{2\gamma^2(k_p - 4k_0)}{\gamma^2(-6k_0 + k_p + 2\lambda_{\pm}) \pm \sqrt{8\gamma^2k_0^2\lambda_{\pm}^2 + \gamma^4(-2k_0 + k_p + 2\lambda_{\pm})^2 + 8\gamma^6}}. \tag{B78}$$

Thus, we have an analytical expression for classical current in the case of two different baths at each boundary of the network.

### B.3 Temperature Dependence of Low-Temperature $\langle J_{\Pi} \rangle$

Here, we analyse the temperature dependence of the quantum current  $\langle J_{\Pi} \rangle$ , obtained when two different baths are coupled at each boundary of the system. From the above analysis, we know that the symmetric part of the quantum current can be expressed as:

$$\langle J_{\Pi} \rangle^s = \frac{\hbar^2 \Delta T}{8\pi k_B T^2 \sqrt{m_0}} \int_0^{\pi} dq \left[ \frac{\gamma^2 \lambda_+^2 \sin^2(q) \sqrt{4k_0 - m_0 \omega_s^2}}{\Lambda_+ - \gamma^2 \lambda_+ (\cos q) (2k_0 - m_0 \omega_s^2)} \omega_s^2 \operatorname{csch}^2 \left( \frac{\hbar \omega_s}{2k_B T} \right) \right]. \tag{B79}$$

Here,  $m_0 \omega_s^2 = k_p + 4\lambda_+ \sin^2(q/2)$ . In the small  $q$  limit, this expression simplifies to:

$$\begin{aligned} \langle J_{\Pi} \rangle^s &= \frac{\hbar^2 \Delta T}{8\pi k_B T^2 \sqrt{m_0}} \int_0^{\pi} dq \left[ \frac{\gamma^2 \lambda_+^2 q^2 \sqrt{4k_0 - k_p - \lambda_+ q^2}}{\Lambda_+ - \gamma^2 \lambda_+ (1 - q^2/2) (2k_0 - k_p - \lambda_+ q^2)} \right. \\ &\quad \left. \times \left( \frac{k_p}{m_0} + \frac{\lambda_+ q^2}{m_0} \right) 4e^{-\frac{\hbar \omega_0}{k_B T}} e^{-\frac{\lambda_+ q^2}{2k_B T m_0 \omega_0}} \right]. \end{aligned} \tag{B80}$$

Following the similar arguments as in Appendix A, for  $k_p \neq 0$ , from Eq. B80 we get the leading-order  $T$ -dependence as:

$$\langle J_{\Pi} \rangle^s \sim \frac{e^{-\frac{\hbar \omega_0}{k_B T}}}{\sqrt{T}} \quad \text{with} \quad \omega_0 = \sqrt{\frac{k_p}{m_0}}. \tag{B81}$$

Now, to understand the temperature dependence of the current when  $k_p = 0$ , we notice that the denominator in the integrand in Eq. B79 for small  $q$  limit takes the form:

$$(\gamma^2 - k_0 \lambda_+)^2 + (k_0 \lambda_+ \gamma^2 + \gamma^2 \lambda_+^2) q^2. \tag{B82}$$

Thus, analytically, we get  $\langle J_{\Pi} \rangle^s \sim T$ , when  $\gamma^2 = k_0 \lambda_+$  and  $\langle J_{\Pi} \rangle^s \sim T^3$  when  $\gamma^2 \neq k_0 \lambda_+$ . Similar results hold for anti-symmetric part of the quantum current  $\langle J_{\Pi} \rangle^a$ . However, it is only defined in the regular regime, where the anti-symmetric frequencies are real. Thus, for  $k_p = 0$ , the total quantum current  $\langle J_{\Pi} \rangle \sim T$  if either  $\gamma^2 = k_0 \lambda_+$  or  $\gamma^2 = k_0 \lambda_-$ . On the other hand, if  $\gamma^2 \neq k_0 \lambda_+ \neq k_0 \lambda_-$ , then  $\langle J_{\Pi} \rangle \sim T^3$ . We are able to reproduce these results numerically.

### Appendix C Two Ohmic Baths at Each Boundary

In this appendix, we consider the case where two types of oscillators at each end of the network are connected to two different Ohmic baths. The Ohmic baths are modeled by white noise, implying that the noises are uncorrelated at different times, leading to Markovian dynamics. Thus, in this case, the self energy of the baths are given by the expression  $\Sigma_{L/R}^+(\omega) = i\gamma_{L/R}^o\omega$  (we assume both baths have the same coupling  $\gamma_L^{o(1)} = \gamma_L^{o(2)} = \gamma_L^o$ ). We write down the EOM for the network variables as:

$$\begin{aligned} m_0\ddot{y}_{\alpha,1} &= -k_p(y_{\alpha,1}) - k[(2y_{\alpha,1} - y_{\alpha,2}) + \lambda(2y_{\beta,1} - y_{\beta,2})] - \gamma_L^o\dot{y}_{\alpha,1} + \eta_{\alpha,L}, \\ m_0\ddot{y}_{\alpha,N} &= -k_p(y_{\alpha,N}) - k[(2y_{\alpha,N} - y_{\alpha,N-1}) \\ &\quad + \lambda(2y_{\beta,N} - y_{\beta,N-1})] - \gamma_R^o\dot{y}_{\alpha,N} + \eta_{\alpha,R}. \end{aligned} \tag{C83}$$

Here,  $\alpha \neq \beta$  and  $\alpha, \beta = 1, 2$ , and  $\eta_{\alpha,L/R}$  represent the noises. Next, we rewrite these EOM in terms of symmetric and anti-symmetric variables ( $y_{s/a,n} = (y_{1,n} \pm y_{2,n})/\sqrt{2}$ ). The symmetric variables at the boundaries satisfy the EOM:

$$\begin{aligned} m_0\ddot{y}_{s,1} &= -k_p(y_{s,1}) - k[(2y_{s,1} - y_{s,2}) + \lambda(2y_{s,1} - y_{s,2})] - \gamma_L^o\dot{y}_{s,1} + \eta_{s,L}, \\ m_0\ddot{y}_{s,N} &= -k_p(y_{s,N}) - k[(2y_{s,N} - y_{s,N-1}) \\ &\quad + \lambda(2y_{s,N} - y_{s,N-1})] - \gamma_R^o\dot{y}_{s,N} + \eta_{s,R}. \end{aligned} \tag{C84}$$

Similarly, the anti-symmetric variables at the boundaries satisfy the EOM:

$$\begin{aligned} m_0\ddot{y}_{a,1} &= -k_p(y_{a,1}) - k[(2y_{a,1} - y_{a,2}) - \lambda(2y_{a,1} - y_{a,2})] - \gamma_L^o\dot{y}_{a,1} + \eta_{a,L}, \\ m_0\ddot{y}_{a,N} &= -k_p(y_{a,N}) - k[(2y_{a,N} - y_{a,N-1}) \\ &\quad - \lambda(2y_{a,N} - y_{a,N-1})] - \gamma_R^o\dot{y}_{a,N} + \eta_{a,R}. \end{aligned} \tag{C85}$$

The remaining symmetric and anti-symmetric variables  $y_{s/a,n}$  (for  $n = 2, \dots, N-1$ ) satisfy the EOM:

$$\begin{aligned} m_0\ddot{y}_{s/a,n} &= -k_p y_{s/a,n} - k[(2y_{s/a,n} - y_{s/a,n-1} - y_{s/a,n+1}) \\ &\quad \pm \lambda(2y_{s/a,n} - y_{s/a,n+1} - y_{s/a,n-1})]. \end{aligned} \tag{C86}$$

In terms of the Fourier modes in frequency domain, the EOM for the boundary variables become:

$$\begin{aligned} z_{L,+}\tilde{y}_{s,1}(\omega) - k(1 + \lambda)\tilde{y}_{s,2}(\omega) &= \tilde{\eta}_{s,L}, \\ z_{R,+}\tilde{y}_{s,N}(\omega) - k(1 + \lambda)\tilde{y}_{s,N-1}(\omega) &= \tilde{\eta}_{s,R}, \\ z_{L,-}\tilde{y}_{a,1}(\omega) - k(1 - \lambda)\tilde{y}_{a,2}(\omega) &= \tilde{\eta}_{a,L}, \\ z_{R,-}\tilde{y}_{a,N}(\omega) - k(1 - \lambda)\tilde{y}_{a,N-1}(\omega) &= \tilde{\eta}_{a,R}. \end{aligned} \tag{C87}$$

Here,  $z_{L/R,+} = (-m_0\omega^2 + k_p + 2k(1 + \lambda) - i\gamma_{L/R}^o\omega)$  and  $z_{L/R,-} = (-m_0\omega^2 + k_p + 2k(1 - \lambda) - i\gamma_{L/R}^o\omega)$ .

#### C.1 Linear Response Heat Current

We define the heat current as the rate of work done by the left baths on the network, which takes the form:

$$J_{II}^W = -[\dot{y}_{1,1}(-\gamma_L^o\dot{y}_{1,1} + \eta_{1,L}) + \dot{y}_{2,1}(-\gamma_L^o\dot{y}_{2,1} + \eta_{2,L})]. \tag{C88}$$

In terms of symmetric and anti-symmetric variables, the current becomes

$$J_{II}^W = -\eta_{s,L}\dot{y}_{s,1} - \eta_{a,L}\dot{y}_{a,1} + \gamma_L^o(\dot{y}_{s,1}^2 + \dot{y}_{a,1}^2). \tag{C89}$$

Now going to the Fourier modes in frequency domain, we express the noise averaged heat current as:

$$\langle J_{II}^W \rangle = \int_{-\infty}^{\infty} d\omega \int_{-\infty}^{\infty} d\omega' e^{-i(\omega+\omega')t} \left\{ i\omega \tilde{y}_{s,1}(\omega) \tilde{\eta}_{s,L}(\omega') + \gamma_L^o i\omega i\omega' \tilde{y}_{s,1}(\omega) \tilde{y}_{s,1}(\omega') \right. \\ \left. + i\omega \tilde{y}_{a,1}(\omega) \tilde{\eta}_{a,L}(\omega') + \gamma_L^o i\omega i\omega' \tilde{y}_{a,1}(\omega) \tilde{y}_{a,1}(\omega') \right\}. \tag{C90}$$

From the EOM in Eq. C87, we notice that

$$\tilde{y}_{s/a,1} = [\tilde{G}^{s/a}]_{1,1} \left( \frac{\tilde{\eta}_{1,L} \pm \tilde{\eta}_{2,L}}{\sqrt{2}} \right) + [\tilde{G}^{s/a}]_{1,N} \left( \frac{\tilde{\eta}_{1,R} \pm \tilde{\eta}_{2,R}}{\sqrt{2}} \right), \\ \tilde{y}_{s/a,N} = [\tilde{G}^{s/a}]_{N,1} \left( \frac{\tilde{\eta}_{1,L} \pm \tilde{\eta}_{2,L}}{\sqrt{2}} \right) + [\tilde{G}^{s/a}]_{N,N} \left( \frac{\tilde{\eta}_{1,R} \pm \tilde{\eta}_{2,R}}{\sqrt{2}} \right). \tag{C91}$$

Here,  $\tilde{G}^{s/a}$  are the inverses of the matrices  $Z^{s,a}$  defined as:

$$Z^{s/a} = \begin{bmatrix} z_{L,\pm} & -\lambda_{\pm} & 0 & \dots & 0 \\ -\lambda_{\pm} & z_{\pm} & -\lambda_{\pm} & \ddots & \vdots \\ \vdots & \ddots & \ddots & \ddots & \vdots \\ \vdots & & \ddots & \ddots & \vdots \\ \vdots & & & -\lambda_{\pm} & z_{\pm} & -\lambda_{\pm} \\ 0 & \dots & \dots & & -\lambda_{\pm} & z_{R,\pm} \end{bmatrix}, \tag{C92}$$

where,  $z_{b,\pm} = -m_0\omega^2 + k_p + 2\lambda_{\pm} - i\gamma_b^o\omega$  and  $z_{\pm} = -m_0\omega^2 + k_p + 2\lambda_{\pm}$ . Recall  $\lambda_{\pm} = k(1 \pm \lambda)$  and they correspond to  $Z^s$  and  $Z^a$ , respectively. The noise average can be computed using the fluctuation-dissipation relation for the Ohmic baths:

$$\langle \tilde{\eta}_{a,b}(\omega) \tilde{\eta}_{a',b'}(\omega') \rangle = \frac{\gamma_b^o \hbar \omega}{\pi} (1 + f_b) \delta_{b,b'} \delta_{a,a'} \delta(\omega + \omega'). \tag{C93}$$

Here,  $a, a' = 1, 2$  and  $b = L, R$ . As explained in previous appendices, finding the left and right parts of the current and combining them, we derive the expression for total current:

$$\langle J_{II}^W \rangle = \int_{-\infty}^{\infty} d\omega \left[ (|[\tilde{G}^s(\omega)]_{1,N}|^2 + |[\tilde{G}^a(\omega)]_{1,N}|^2) \right. \\ \left. \times \gamma_L^o \gamma_R^o \frac{\hbar \omega^3}{\pi} (f_L - f_R) \right] = \langle J_{II}^W \rangle^s + \langle J_{II}^W \rangle^a. \tag{C94}$$

In the linear response regime, this heat current takes the form:

$$\langle J_{II}^W \rangle = \frac{k_B \Delta T}{\pi} \int_{-\infty}^{\infty} d\omega \left[ (|[\tilde{G}^s(\omega)]_{1,N}|^2 + |[\tilde{G}^a(\omega)]_{1,N}|^2) \right. \\ \left. \times \gamma_L^o \gamma_R^o \omega^2 \left( \frac{\hbar \omega}{2k_B T} \right)^2 \operatorname{csch}^2 \left( \frac{\hbar \omega}{2k_B T} \right) \right]. \tag{C95}$$

Next, we find an analytical expression for the current in the thermodynamic limit for large temperature.

### C.2 Thermodynamic Limit and Analytical Expression for Classical Heat Current

As explained in previous appendices, to find the analytical expression for classical current, we need to manipulate large  $N$  properties of the matrix  $Z^{s/a} = \lambda_{\pm} \tilde{Z}^{s/a}$ . Given  $N$  number of lattice sites in the network,  $\tilde{Z}^{s/a}$  are  $N \times N$  tridiagonal matrices whose offdiagonal elements are  $-1$  and diagonal elements excluding the first and last one are  $(-m_0\omega^2 + k_p)/\lambda_{+,-} + 2$ , respectively. The first and last diagonal elements of  $\tilde{Z}^s$  are  $z_{L,+}/\lambda_+$  and  $z_{R,+}/\lambda_+$ , respectively, and those for  $\tilde{Z}^a$  are  $z_{L,-}/\lambda_-$  and  $z_{R,-}/\lambda_-$ , respectively. The expression for heat current in Eq. C94 involves matrix elements  $[\tilde{G}^{s/a}]_{1,N}$ , which is given by the inverse of  $Z^{s/a}$ :  $\tilde{G}^{s/a} = (Z^{s/a})^{-1} = (\tilde{Z}^{s/a})^{-1}/\lambda_{\pm}$ . Here,  $\lambda_{\pm}$  appear in the expressions for  $\tilde{G}^s$  and  $\tilde{G}^a$ , respectively. Thus, we have

$$|\tilde{G}^{s/a}_{1,N}| = \frac{1}{\lambda_{\pm} |\det \tilde{Z}^{s/a}|}. \tag{C96}$$

We simplify the determinant of the tridiagonal matrices  $\tilde{Z}^{s/a}$  in the large  $N$  limit to get an analytical expression. Choosing  $\gamma^o_L = \gamma^o_R = \gamma^o$ , we find the expression for classical current as

$$\langle J_{\Pi}^{wcl} \rangle = \frac{k_B \Delta T}{\pi} \int_{-\infty}^{\infty} d\omega (\gamma^o)^2 \omega^2 (|\tilde{G}^{s/a}_{1,N}|^2 + |\tilde{G}^a_{1,N}|^2) = \langle J_{\Pi}^{wcl} \rangle^s + \langle J_{\Pi}^{wcl} \rangle^a. \tag{C97}$$

To follow a similar derivation as done in Appendix B, we define  $\tilde{a}_{\pm} = ((-m_0\omega^2 + k_p)/\lambda_{\pm}) + 2$  and  $\epsilon_{L,R} = i\omega\gamma^o_{L/R}/\lambda_{\pm}$  for  $\tilde{Z}^s$  and  $\tilde{Z}^a$ , respectively. Now with the substitution  $\tilde{a}_{\pm} = 2 \cos q$ , in the large  $N$  limit (see Eq. A35), we re-express the symmetric and anti-symmetric parts of the classical current in the form:

$$\langle J_{\Pi}^{wcl} \rangle^{s/a} = \frac{k_B \Delta T}{\pi} \int_0^{\pi} dq \frac{g_1^{s/a}(q)}{(1 - g_2^{s/a}(q)^2)^{1/2}}, \tag{C98}$$

where, the integrand is given explicitly as:

$$\frac{g_1^{s/a}(q)}{(1 - g_2^{s/a}(q)^2)^{1/2}} = \frac{\gamma^o \lambda_{\pm}^2}{m_0} \frac{\sin^2(q)}{\Lambda_{s/a} - \zeta_{s/a} \cos(q)}. \tag{C99}$$

Here,

$$\Lambda_{s/a} = \lambda_{\pm}^2 + \frac{(k_p + 2\lambda_{\pm})(\gamma^o)^2}{m_0} \quad \text{and} \quad \zeta_{s/a} = \frac{2\lambda_{\pm}(\gamma^o)^2}{m_0}. \tag{C100}$$

Thus, the expression for the classical current is

$$\begin{aligned} \langle J_{\Pi}^{wcl} \rangle &= \langle (J_{\Pi}^w)^{cl} \rangle^s + \langle (J_{\Pi}^w)^{cl} \rangle^a \\ &= \frac{\gamma^o k_B \Delta T}{m_0} \left( \frac{\lambda_+^2}{\zeta_s^2} (\Lambda_s - \sqrt{\Lambda_s^2 - \zeta_s^2}) + \frac{\lambda_-^2}{\zeta_a^2} (\Lambda_a - \sqrt{\Lambda_a^2 - \zeta_a^2}) \right). \end{aligned} \tag{C101}$$

### C.3 Temperature Dependence of Low-Temperature $\langle J_{\Pi}^w \rangle$

Now, we analyse the temperature dependence of the low-temperature quantum heat current in Eq. C94. In order to understand the role of pinning strength on the temperature dependence, we analyse two different cases, one with  $k_p \neq 0$  and the other with  $k_p = 0$ .

We notice that for  $N \rightarrow \infty$ , in the linear response regime, the symmetric part of the quantum current is

$$\langle J_{\Pi}^w \rangle^s = \frac{\gamma^o \lambda_+^2 \hbar^2 \Delta T}{4\pi m_0 k_B T^2} \int_0^\pi \frac{dq \sin^2 q \omega^2}{\Lambda_s - \zeta_s \cos q} \operatorname{csch}^2 \left( \frac{\hbar \omega}{2k_B T} \right). \tag{C102}$$

Here,  $\omega^2 = (k_p + 4\lambda_+ \sin^2(q/2))/m_0$ . As explained in the previous appendices, by taking the small  $q$  limit to understand the temperature dependence of the quantum current for  $k_p \neq 0$ , we find

$$\langle J_{\Pi}^w \rangle^s \approx \frac{\gamma^o \lambda_+^2 \hbar^2 \Delta T}{4\pi m_0 k_B T^2} \int_0^\pi \left[ \frac{dq q^2}{\Lambda_s - \zeta_s (1 - q^2/2)} \left( \frac{k_p}{m_0} + \frac{\lambda_+ q^2}{m_0} \right) 4e^{-\frac{\hbar \omega_0}{k_B T}} e^{-\frac{\hbar \lambda_+ q^2}{2k_B T m_0 \omega_0}} \right], \tag{C103}$$

where  $\omega_0 = \sqrt{k_p/m_0}$ . By substituting  $x = (\hbar \lambda_+ q^2)/(2m_0 \omega_0 k_B T)$ , we obtain the leading-order  $T$ -dependence:  $\langle J_{\Pi}^w \rangle^s \sim (e^{-\hbar \omega_0/(k_B T)})/\sqrt{T}$ .

For  $k_p = 0$ , we have  $\Lambda_s = \lambda_+^2 + \zeta_s$  and  $\omega^2 \approx \lambda_+ q^2/m_0$  in the small  $q$  limit. Thus, we find

$$\langle J_{\Pi}^w \rangle^s \approx \frac{\gamma^o \lambda_+^2 \hbar^2 \Delta T}{4\pi m_0 k_B T^2} \int_0^\pi dq \left[ \frac{q^2}{\lambda_+^2 + \zeta_s (q^2/2)} \times \frac{\lambda_+ q^2}{m_0} \operatorname{csch}^2 \left( \frac{\hbar \omega}{2k_B T} \right) \right]. \tag{C104}$$

By substituting  $x = \hbar \omega/(2k_B T)$ , and noticing that  $\omega \propto q$ , we get the leading order  $T$ -dependence  $\langle J_{\Pi}^w \rangle^s \sim T^3$ . These observations agree with the results already known from the heat transport of ordered harmonic lattices [38]. Similar temperature dependence holds for the anti-symmetric part of the current  $\langle J_{\Pi}^w \rangle^a$  as well. However, this current is bounded only in the regular regime.

### C.4 Comparison of Classical Heat Current for Rubin Bath and Ohmic Bath

We compare the classical heat currents obtained for heat baths with different spectral properties. To compare the analytical expressions for classical currents obtained through

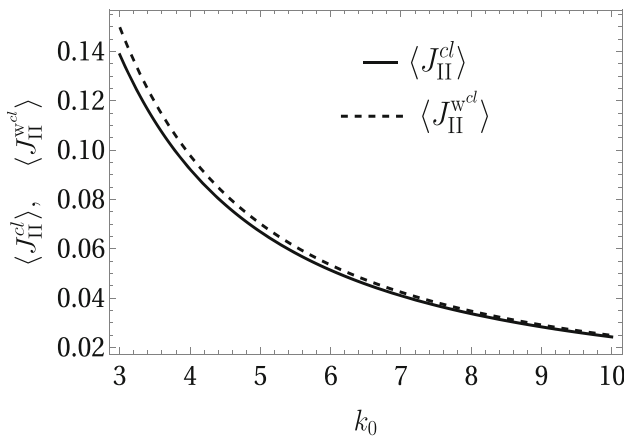


**Fig. 6** Comparison between the classical heat currents  $\langle J_{\Pi}^{cl} \rangle$  and  $\langle J_{\Pi}^{w,cl} \rangle$  as a function of the bath spring constant  $k_0$ . The y-axis represents the heat currents multiplied by the common factor  $\pi/(k_B \Delta T)$ . We set the parameters  $\lambda = 0.7$ ,  $\gamma = 0.5k$ ,  $k_p = 0$  and  $m_0 = k = \hbar = k_B = 1$  in the numerical analysis

Rubin baths to that of Ohmic baths, we notice that the coupling strengths  $\gamma$  and  $\gamma^o$  should satisfy the condition:

$$\gamma^o = \frac{\sqrt{m_0}\gamma^2}{k_0^{3/2}}. \tag{C105}$$

This identity is obtained by comparing the self energies  $\tilde{\Sigma}^+(\omega)$  of both types of baths at small frequencies. We notice that the values of current become almost equal as we increase the value of  $k_0$  as shown in Fig. 6. This behavior is expected, as Rubin baths with higher bandwidths exhibit properties resembling Ohmic baths (See [51] for a detailed analysis).

### Appendix D Single Ohmic Bath at Each Boundary

In this appendix, we consider the case where two types of oscillators at each end of the network are connected to a single Ohmic bath. We write down the EOM for the network variables as:

$$\begin{aligned} m_0\ddot{y}_{\alpha,1} &= -k_p y_{\alpha,1} - k [2y_{\alpha,1} - y_{\alpha,2} + \lambda(2y_{\beta,1} - y_{\beta,2})] - \gamma_L^o(\dot{y}_{\alpha,1} + \dot{y}_{\beta,1}) + \eta_L, \\ m_0\ddot{y}_{\alpha,N} &= -k_p y_{\alpha,N} - k [2y_{\alpha,N} - y_{\alpha,N-1} + \lambda(2y_{\beta,N} - y_{\beta,N-1})] \\ &\quad - \gamma_R^o(\dot{y}_{\alpha,N} + \dot{y}_{\beta,N}) + \eta_R. \end{aligned} \tag{D106}$$

Here,  $\alpha \neq \beta$  and  $\alpha, \beta = 1, 2$ , and  $\eta_{L/R}$  represent the noises of the left and right baths. We rewrite these EOM in terms of symmetric and anti-symmetric variables ( $y_{s/a,n} = (y_{1,n} \pm y_{2,n})/\sqrt{2}$ ). The symmetric variables at the boundaries satisfy the EOM:

$$\begin{aligned} m_0\ddot{y}_{s,1} &= -k_p y_{s,1} - k [2y_{s,1} - y_{s,2} + \lambda(2y_{s,1} - y_{s,2})] - 2\gamma_L^o \dot{y}_{s,1} + \sqrt{2}\eta_L, \\ m_0\ddot{y}_{s,N} &= -k_p y_{s,N} - k [2y_{s,N} - y_{s,N-1} + \lambda(2y_{s,N} - y_{s,N-1})] \\ &\quad - 2\gamma_R^o \dot{y}_{s,N} + \sqrt{2}\eta_R. \end{aligned} \tag{D107}$$

However, the anti-symmetric variables at the boundaries decouple from the dissipation terms (proportional to  $\gamma_L^o$  and  $\gamma_R^o$ ) as well as the noise terms ( $\eta_L$  and  $\eta_R$ ), and satisfy the EOM:

$$\begin{aligned} m_0\ddot{y}_{a,1} &= -k_p y_{a,1} - k [2y_{a,1} - y_{a,2} - \lambda(2y_{a,1} - y_{a,2})], \\ m_0\ddot{y}_{a,N} &= -k_p y_{a,N} - k [2y_{a,N} - y_{a,N-1} - \lambda(2y_{a,N} - y_{a,N-1})]. \end{aligned} \tag{D108}$$

The remaining symmetric and anti-symmetric variables  $y_{s/a,n}$  (for  $n = 2, \dots, N - 1$ ) satisfy the EOM:

$$\begin{aligned} m_0\ddot{y}_{s/a,n} &= -k_p y_{s/a,n} - k [2y_{s/a,n} - y_{s/a,n-1} - y_{s/a,n+1} \\ &\quad \pm \lambda(2y_{s/a,n} - y_{s/a,n+1} - y_{s/a,n-1})]. \end{aligned} \tag{D109}$$

Thus, we observe that the anti-symmetric modes get entirely decoupled from the bath variables for this type of coupling between the baths and the oscillator network. This implies that the transport depends only on the symmetric modes, allowing for a steady state even beyond the stable regime.

#### D.1 Linear Response Heat Current

We define the heat current as the rate of work done by the left bath on the network, which takes the form:

$$J_1^W = - [\dot{y}_{1,1}(-\gamma_L^o(\dot{y}_{1,1} + \dot{y}_{2,1}) + \eta_L) + \dot{y}_{2,1}(-\gamma_L^o(\dot{y}_{2,1} + \dot{y}_{1,1}) + \eta_L)]. \tag{D110}$$

In terms of symmetric and anti-symmetric variables, the current becomes

$$J_1^w = - \left[ \sqrt{2} \dot{y}_{s,1} (-\sqrt{2} \gamma_L^o \dot{y}_{s,1} + \eta_L) \right]. \tag{D111}$$

Thus, we can see that the current is independent of the anti-symmetric modes and it remains bounded even in the unstable regime of the coupling.

As explained in the previous appendices, we can find the analytical expression for classical heat current and temperature-dependence of the quantum current in this case too. For instance, going to the Fourier modes we can express the current as

$$\langle J_1^w \rangle = \int_{-\infty}^{\infty} d\omega \left[ 4 | [G_s^+(\omega)]_{1,N} |^2 \gamma_L^o \gamma_R^o \omega^2 \frac{\hbar \omega}{\pi} (f_L - f_R) \right]. \tag{D112}$$

Here,  $G_s^+$  is the inverse of the tri-diagonal matrix  $Z$ :

$$Z = \begin{bmatrix} z_{L+} & -\lambda_+ & 0 & \cdots & 0 \\ -\lambda_+ & z_+ & -\lambda_+ & \ddots & \vdots \\ \vdots & \ddots & \ddots & \ddots & \vdots \\ \vdots & & \ddots & \ddots & \vdots \\ \vdots & & & -\lambda_+ & z_+ & -\lambda_+ \\ 0 & \cdots & \cdots & & -\lambda_+ & z_{R+} \end{bmatrix}. \tag{D113}$$

Here,  $z_{b+} = -m_0 \omega^2 + k_p + 2\lambda_+ - i2\gamma_b^o \omega$ ,  $z_+ = -m_0 \omega^2 + k_p + 2\lambda_+$ , and  $\lambda_+ = k(1 + \lambda)$  for  $b = L, R$ . Thus, we obtain the analytical expression for the classical current as

$$\langle J_1^{w,cl} \rangle = \frac{2\gamma^o k_B \Delta T}{m_0} \left( \frac{\lambda_+^2}{\zeta^2} (\Lambda - \sqrt{\Lambda^2 - \zeta^2}) \right), \tag{D114}$$

where  $\Lambda = \lambda_+^2 + (k_p + 2\lambda_+/m^2)4\gamma^2$  and  $\zeta = 8\lambda_+\gamma^2/m$  assuming  $\gamma_L^o = \gamma_R^o = \gamma$ .

**Acknowledgements** We would like to thank A. Clerk and K. Roychowdhury for the insightful discussions.

**Data Availability** The authors declare that the data supporting the findings of this study are available within the paper.

**Declarations**

**Conflict of interest** The authors have no conflict of interest to declare that are relevant for the content of this article.

**References**

1. Hatano, N., Nelson, D.R.: Localization transitions in non-Hermitian quantum mechanics. *Phys. Rev. Lett.* **77**(3), 570–573 (1996). <https://doi.org/10.1103/PhysRevLett.77.570>
2. Bender, C.M., Boettcher, S.: Real spectra in non-Hermitian Hamiltonians having PT symmetry. *Phys. Rev. Lett.* **80**, 5243–5246 (1998). <https://doi.org/10.1103/PhysRevLett.80.5243>
3. Khare, A., Mandal, B.P.: A PT-invariant potential with complex QES eigenvalues. *Phys. Lett. A* **272**(1), 53–56 (2000). [https://doi.org/10.1016/S0375-9601\(00\)00409-6](https://doi.org/10.1016/S0375-9601(00)00409-6)
4. Bagchi, B., Cannata, F., Quesne, C.: PT-symmetric sextic potentials. *Phys. Lett. A* **269**(2), 79–82 (2000). [https://doi.org/10.1016/S0375-9601\(00\)00227-9](https://doi.org/10.1016/S0375-9601(00)00227-9)

5. Mostafazadeh, A.: Pseudo-Hermiticity versus PT symmetry: the necessary condition for the reality of the spectrum of a non-Hermitian Hamiltonian. *J. Math. Phys.* **43**(1), 205–214 (2002). <https://doi.org/10.1063/1.1418246>
6. Bender, C.M., Berry, M.V., Mandilara, A.: Generalized PT symmetry and real spectra. *J. Phys. A* **35**(31), 467 (2002). <https://doi.org/10.1088/0305-4470/35/31/101>
7. Berry, M.V.: Physics of non-Hermitian degeneracies. *Czechoslov. J. Phys.* **54**(10), 1039–1047 (2004). <https://doi.org/10.1023/B:CJOP.0000044002.05657.04>
8. Guo, A., Salamo, G.J., Duchesne, D., Morandotti, R., Volatier-Ravat, M., Aimez, V., Siviloglou, G.A., Christodoulides, D.N.: Observation of PT-symmetry breaking in complex optical potentials. *Phys. Rev. Lett.* **103**, 093902 (2009). <https://doi.org/10.1103/PhysRevLett.103.093902>
9. Heiss, W.D.: The physics of exceptional points. *J. Phys. A* **45**(44), 444016 (2012). <https://doi.org/10.1088/1751-8113/45/44/444016>
10. Rudner, M.S., Levitov, L.S.: Topological transition in a non-Hermitian quantum walk. *Phys. Rev. Lett.* **102**(6), 065703 (2009). <https://doi.org/10.1103/PhysRevLett.102.065703>
11. Liang, S.-D., Huang, G.-Y.: Topological invariance and global Berry phase in non-Hermitian systems. *Phys. Rev. A* **87**(1), 012118 (2013). <https://doi.org/10.1103/PhysRevA.87.012118>
12. Shen, H., Zhen, B., Fu, L.: Topological band theory for non-Hermitian Hamiltonians. *Phys. Rev. Lett.* **120**(14), 146402 (2018). <https://doi.org/10.1103/PhysRevLett.120.146402>
13. Lieu, S.: Topological phases in the non-Hermitian Su–Schrieffer–Heeger model. *Phys. Rev. B* **97**(4), 045106 (2018). <https://doi.org/10.1103/PhysRevB.97.045106>
14. Pan, M., Zhao, H., Miao, P., Longhi, S., Feng, L.: Photonic zero mode in a non-Hermitian photonic lattice. *Nat. Commun.* **9**(1), 1308 (2018). <https://doi.org/10.1038/s41467-018-03822-8>
15. Kawabata, K., Shiozaki, K., Ueda, M., Sato, M.: Symmetry and topology in non-Hermitian physics. *Phys. Rev. X* **9**(4), 041015 (2019). <https://doi.org/10.1103/PhysRevX.9.041015>
16. Wang, K., Dutt, A., Wojcik, C.C., Fan, S.: Topological complex-energy braiding of non-Hermitian bands. *Nature* **598**(7879), 59–64 (2021). <https://doi.org/10.1038/s41586-021-03848-x>
17. Vyas, V.M., Roy, D.: Topological aspects of periodically driven non-Hermitian Su–Schrieffer–Heeger model. *Phys. Rev. B* **103**(7), 075441 (2021). <https://doi.org/10.1103/PhysRevB.103.075441>
18. Nehra, R., Roy, D.: Topology of multipartite non-Hermitian one-dimensional systems. *Phys. Rev. B* **105**, 195407 (2022). <https://doi.org/10.1103/PhysRevB.105.195407>
19. Colpa, J.H.P.: Diagonalization of the quadratic boson Hamiltonian. *Physica A* **93**(3), 327–353 (1978). [https://doi.org/10.1016/0378-4371\(78\)90160-7](https://doi.org/10.1016/0378-4371(78)90160-7)
20. Rossignoli, R., Kowalski, A.M.: Complex modes in unstable quadratic bosonic forms. *Phys. Rev. A* **72**, 032101 (2005). <https://doi.org/10.1103/PhysRevA.72.032101>
21. McDonald, A., Pereg-Barnea, T., Clerk, A.A.: Phase-dependent chiral transport and effective non-Hermitian dynamics in a bosonic Kitaev–Majorana chain. *Phys. Rev. X* **8**, 041031 (2018). <https://doi.org/10.1103/PhysRevX.8.041031>
22. Lieu, S.: Topological symmetry classes for non-Hermitian models and connections to the bosonic Bogoliubov–de Gennes equation. *Phys. Rev. B* **98**, 115135 (2018). <https://doi.org/10.1103/PhysRevB.98.115135>
23. Wang, Y.-X., Clerk, A.A.: Non-Hermitian dynamics without dissipation in quantum systems. *Phys. Rev. A* **99**, 063834 (2019). <https://doi.org/10.1103/PhysRevA.99.063834>
24. Flynn, V.P., Cobanera, E., Viola, L.: Deconstructing effective non-Hermitian dynamics in quadratic bosonic Hamiltonians. *New J. Phys.* **22**(8), 083004 (2020). <https://doi.org/10.1088/1367-2630/ab9e87>
25. Flynn, V.P., Cobanera, E., Viola, L.: Topology by dissipation: majorana bosons in metastable quadratic Markovian dynamics. *Phys. Rev. Lett.* **127**, 245701 (2021). <https://doi.org/10.1103/PhysRevLett.127.245701>
26. Peskin, M.E., Schroeder, D.V.: *An Introduction to Quantum Field Theory*. Addison-Wesley, Reading (1995)
27. Schwartz, M.D.: *Quantum Field Theory and the Standard Model*. Cambridge University Press, Cambridge (2014)
28. Aspelmeyer, M., Kippenberg, T.J., Marquardt, F.: Cavity optomechanics. *Rev. Mod. Phys.* **86**, 1391–1452 (2014). <https://doi.org/10.1103/RevModPhys.86.1391>
29. Barton, G.: Quantum mechanics of the inverted oscillator potential. *Ann. Phys.* **166**(2), 322–363 (1986). [https://doi.org/10.1016/0003-4916\(86\)90142-9](https://doi.org/10.1016/0003-4916(86)90142-9)
30. Subramanian, V., Hegde, S.S., Vishveshwara, S., Bradlyn, B.: Physics of the inverted harmonic oscillator: From the lowest Landau level to event horizons. *Ann. Phys.* **435**, 168470 (2021). <https://doi.org/10.1016/j.aop.2021.168470>
31. Lepri, S., Livi, R., Politi, A.: Thermal conduction in classical low-dimensional lattices. *Phys. Rep.* **377**(1), 1 (2003). [https://doi.org/10.1016/S0370-1573\(02\)00558-6](https://doi.org/10.1016/S0370-1573(02)00558-6)



32. Dhar, A.: Heat transport in low-dimensional systems. *Adv. Phys.* **57**(5), 457–537 (2008). <https://doi.org/10.1080/00018730802538522>
33. Xu, G., Zhou, X., Li, Y., Cao, Q., Chen, W., Xiao, Y., Yang, L., Qiu, C.-W.: Non-Hermitian chiral heat transport. *Phys. Rev. Lett.* **130**, 266303 (2023). <https://doi.org/10.1103/PhysRevLett.130.266303>
34. Dhar, A., Roy, D.: Heat transport in harmonic lattices. *J. Stat. Phys.* **125**(4), 801–820 (2006). <https://doi.org/10.1007/s10955-006-9235-3>
35. Ali, T., Bhattacharyya, A., Haque, S.S., Kim, E.H., Moynihan, N., Murugan, J.: Chaos and complexity in quantum mechanics. *Phys. Rev. D* **101**, 026021 (2020). <https://doi.org/10.1103/PhysRevD.101.026021>
36. Bhattacharyya, A., Chemissany, W., Haque, S.S., Murugan, J., Yan, B.: The multi-faceted inverted harmonic oscillator: chaos and complexity. *SciPost Phys. Core* **4**, 002 (2021). <https://doi.org/10.21468/SciPostPhysCore.4.1.002>
37. Qu, L.-C., Chen, J., Liu, Y.-X.: Chaos and complexity for inverted harmonic oscillators. *Phys. Rev. D* **105**, 126015 (2022). <https://doi.org/10.1103/PhysRevD.105.126015>
38. Roy, D., Dhar, A.: Heat transport in ordered harmonic lattices. *J. Stat. Phys.* **131**(3), 535–541 (2008). <https://doi.org/10.1007/s10955-008-9487-1>
39. Dhar, A.: Heat conduction in the disordered harmonic chain revisited. *Phys. Rev. Lett.* **86**, 5882–5885 (2001). <https://doi.org/10.1103/PhysRevLett.86.5882>
40. Roy, D., Dhar, A.: Role of pinning potentials in heat transport through disordered harmonic chains. *Phys. Rev. E* **78**, 051112 (2008). <https://doi.org/10.1103/PhysRevE.78.051112>
41. Chaudhuri, A., Kundu, A., Roy, D., Dhar, A., Lebowitz, J.L., Spohn, H.: Heat transport and phonon localization in mass-disordered harmonic crystals. *Phys. Rev. B* **81**, 064301 (2010). <https://doi.org/10.1103/PhysRevB.81.064301>
42. Rubin, R.J., Greer, W.L.: Abnormal lattice thermal conductivity of a one-dimensional, harmonic, isotopically disordered crystal. *J. Math. Phys.* **12**(8), 1686–1701 (1971). <https://doi.org/10.1063/1.1665793>
43. Casher, A., Lebowitz, J.L.: Heat flow in regular and disordered harmonic chains. *J. Math. Phys.* **12**(8), 1701–1711 (1971). <https://doi.org/10.1063/1.1665794>
44. Hu, G.Y., O’Connell, R.F.: Analytical inversion of symmetric tri-diagonal matrices. *J. Phys. A* **29**(7), 1511 (1996). <https://doi.org/10.1088/0305-4470/29/7/020>
45. Liu, X., Gupta, S.D., Agarwal, G.S.: Regularization of the spectral singularity in *mathcal{PT}*-symmetric systems by all-order nonlinearities: Nonreciprocity and optical isolation. *Phys. Rev. A* **89**, 013824 (2014). <https://doi.org/10.1103/PhysRevA.89.013824>
46. Roy, D.: Crossover from fermi-pasta-ulam to normal diffusive behavior in heat conduction through open anharmonic lattices. *Phys. Rev. E* **86**, 041102 (2012). <https://doi.org/10.1103/PhysRevE.86.041102>
47. Bondyopadhyaya, N., Roy, D.: Nonequilibrium electrical, thermal and spin transport in open quantum systems of topological superconductors, semiconductors and metals. *J. Stat. Phys.* **187**, 11 (2022). <https://doi.org/10.1007/s10955-022-02902-w>
48. Jonsson, R.H., Hackl, L., Roychowdhury, K.: Entanglement dualities in supersymmetry. *Phys. Rev. Res.* **3**, 023213 (2021). <https://doi.org/10.1103/PhysRevResearch.3.023213>
49. Zhang, X.-L., Wang, S., Hou, B., Chan, C.T.: Dynamically encircling exceptional points: in situ control of encircling loops and the role of the starting point. *Phys. Rev. X* **8**, 021066 (2018). <https://doi.org/10.1103/PhysRevX.8.021066>
50. Nehra, R., Roy, D.: Anomalous dynamical response of non-Hermitian topological phases. *Phys. Rev. B* **109**, 094311 (2024). <https://doi.org/10.1103/PhysRevB.109.094311>
51. Das, A., Dhar, A., Santra, I., Satpathi, U., Sinha, S.: Quantum Brownian motion: Drude and ohmic baths as continuum limits of the Rubin model. *Phys. Rev. E* **102**, 062130 (2020). <https://doi.org/10.1103/PhysRevE.102.062130>

**Publisher’s Note** Springer Nature remains neutral with regard to jurisdictional claims in published maps and institutional affiliations.

Springer Nature or its licensor (e.g. a society or other partner) holds exclusive rights to this article under a publishing agreement with the author(s) or other rightsholder(s); author self-archiving of the accepted manuscript version of this article is solely governed by the terms of such publishing agreement and applicable law.